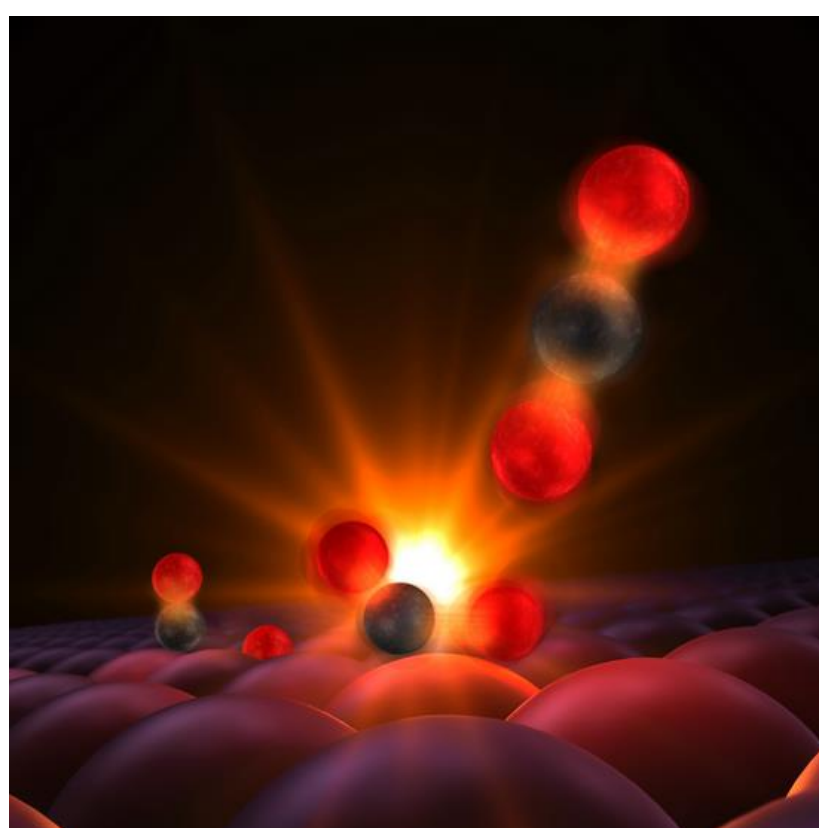
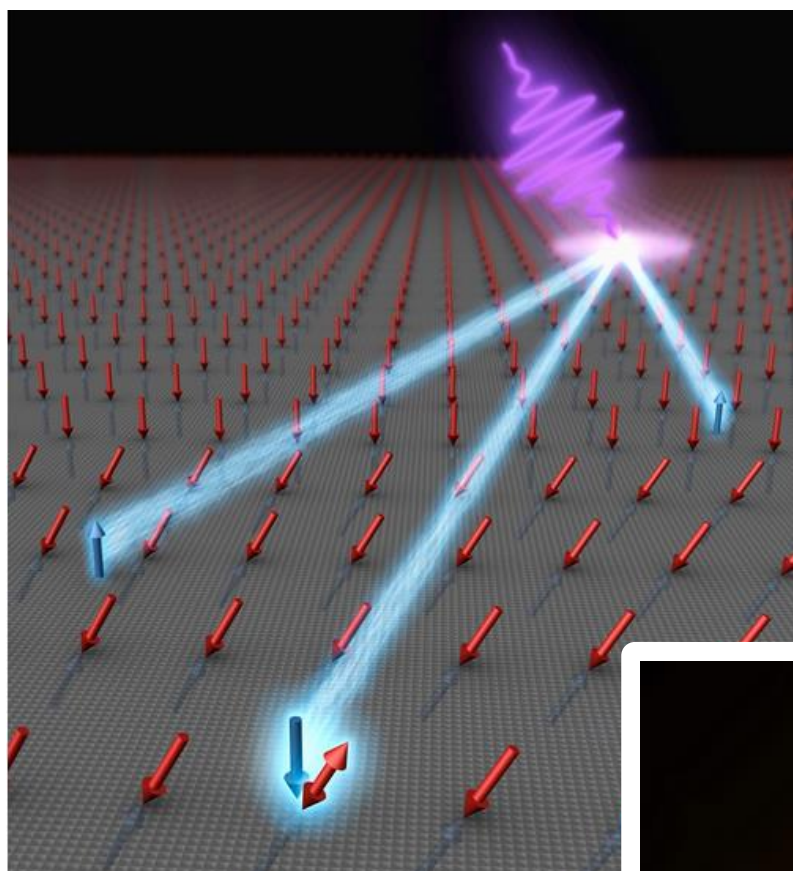


# The Soft X-ray Laser @ MAX IV

## *A Science Case for SXL*





# The Soft X-ray Laser @ MAX IV

---

## A Science Case for SXL

### The Working Group

Anders Nilsson	Stockholm University, Chair	
Stefano Bonetti	Stockholm University, Co-chair	Condensed Matter
Henrik Öström	Stockholm University	Chemistry
Michael Odelius	Stockholm University	Chemistry
Mats Larsson	Stockholm University	FEL and AMO Science
Oscar Tjernberg	KTH	Condensed Matter
Jonas Sellberg	KTH	Life Science
Jan-Erik Rubensson	Uppsala University	AMO Science
Vitaliy Goryashko	Uppsala University	FEL Science
Raimund Feifel	Gothenburg University	AMO Science
Richard Neutze	Gothenburg University	Life Science
Per Johnsson	Lund University	AMO Science
Sverker Werin	Lund University	FEL Science
Francesca Curbis	Lund University	FEL Science
Jesper Andersen	MAX IV Laboratory	Observer

Cover illustrations reprinted by permission from  
SLAC National Accelerator Laboratory.

## **Authors**

Katrin Amann-Winkel, Magnus H. Berntsen, Olle Björneholm, Stefano Bonetti, Gisela Brändén, Yi-De Chuang, Martina Dell'Angela, Hermann Dürr, Raimund Feifel, Alexander Föhlisch, Markus Guehr, Greger Hammarin, Johan Hellsvik, Steve Johnson, Per Johnsson, Olof Jönsson, Victor Kimberg, Maya Kiskinova, Lars Kloo, Filipe Maia, Kess Marks, Claudio Masciovecchio, Anders Mikkelsen, Chris Milne, Richard Neutze, Anders Nilsson, Dennis Nordlund, Michael Odelius, Hirohito Ogasawara, Fivos Perakis, Lars G.M. Pettersson, Håkan Rensmo, Marcel Reutzel, Jan-Erik Rubensson, Peter Salén, Joachim Schnadt, Simon Schreck, Jonas Sellberg, Joachim Stöhr, Nicusor Timneanu, Oscar Tjernberg, Philippe Wernet, Henrik Öström.

## TABLE OF CONTENTS

<b>1.</b>	<b>Introduction</b>	<b>4</b>
<b>2.</b>	<b>Short Outline of the SXL Beamline</b>	<b>6</b>
2.1	The MAX IV facility as SXL driver	6
2.2	Tentative performance of the SXL	7
2.3	Some possible features of the SXL on MAX IV	8
2.4	Possible layout	10
<b>3.</b>	<b>Unique Characteristics of SXL</b>	<b>13</b>
3.1	Bridging the spectral gap – a broadband sub-fs pump facility	13
3.2	Unique detection schemes	16
3.3	Imaging for life science and condensed matter	17
<b>4.</b>	<b>AMO Science</b>	<b>21</b>
4.1	Ultrafast charge and structural dynamics	21
4.2	Nonlinear X-ray AMO	22
<b>5.</b>	<b>Chemistry</b>	<b>27</b>
5.1	Photochemistry	27
5.2	Heterogeneous catalysis	30
5.3	Electrochemistry	31
5.4	Photovoltaics	33
<b>6.</b>	<b>Condensed Matter Physics</b>	<b>36</b>
6.1	Ultrafast magnetism: watching spins move in time and space	37
6.2	Correlated systems - Superconductors	39
6.3	Correlated systems - Multiferroics	40
6.4	Structure and dynamics of liquids and glasses	42
6.5	Semiconductor nanostructure dynamics: Dopants and interfaces	44
6.6	Sub-femtosecond opportunities in condensed matter	46
<b>7.</b>	<b>Life Science</b>	<b>50</b>
7.1	Coherent diffractive imaging of living cells and other intrinsically heterogeneous biological building blocks	51
7.2	Fluctuation-based X-ray scattering of conformational changes in protein solutions	52
7.3	Energy conversion involving non-adiabatic dynamics probed by ultrafast X-ray spectroscopy	54
<b>8.</b>	<b>Theory Support for New Experiments</b>	<b>58</b>
8.1	Methods development	58
	<b>Appendix</b>	<b>62</b>
A.	The SXL workshop	62
A.1	Pictures	62
A.2	Program	63
A.3	Participants	65
B.	Glossary	69

# 1. Introduction

---

Sweden has a strong X-ray community and created the first Swedish synchrotron radiation (SR) facility as MAX-lab already in the 1980s. Since then several steps have been taken to build a more advanced SR machine in terms of MAX II and now soon to come into operation MAX IV. The latter machine will become the brightest SR source in the world and the anticipation of an excellent scientific program is very high with a broad scope ranging from biology to atomic physics. With the development of the Free electron LASer in Hamburg (FLASH) and the Linac Coherent Light Source (LCLS) at Stanford a new class of X-ray laser sources has become realized with ultrashort pulses down to a few femtoseconds, extreme peak brightness and high coherence that have opened-up for new types of experiments in the time domain and in coherent imaging. It is essential that Sweden can maintain to be part of the forefront of X-ray science in the world by complementing the outstanding MAX IV SR source with also X-ray laser capabilities.

There is an extraordinary opportunity to build a Soft X-ray Laser (SXL) beamline at the existing MAX IV facility that can generate free electron laser (FEL) properties between 250-1000 eV. This would build on already made investments in the short pulse linear accelerator (linac) as well as existing buildings that will be used, and capitalize on movable experimental stations at soft X-ray beamlines and the general infrastructure at MAX IV (see fig. 1.1). It can be constructed with a modest investment and will get Sweden started with FEL science. In the Swedish tradition, future steps with other beamlines that would extend the X-ray laser capabilities into the hard X-ray regime can then follow this. Sweden has a strong soft X-ray tradition that will become enhanced with SXL, which could be designed to have unique characteristics in alignment with Swedish research interests. Furthermore, the scientific program can be directly connected to several of the soft X-ray beamlines at MAX IV such as VERITAS, HIPPIE, SoftiMAX etc.



**Figure 1.1.** Aerial picture of the MAX IV facility under construction with depiction in orange where the SXL beamline would be located after the 3 GeV linear accelerator. In shaded orange is indicated future expansion possibilities.

With the goal to create the science case for SXL, a working group with representatives of most major Swedish universities was created during the fall of 2015. The working group is co-chaired by Anders Nilsson and Stefano Bonetti at Stockholm University. In order to explore the scientific interest in Sweden for the SXL beamline and make an inventory of what science could be conducted a workshop was organized in Stockholm at the AlbaNova University Center March 21-23 2016. The top scientists in the world currently using soft X-ray lasers to conduct experiments, leading FEL accelerator scientists and representatives of all major soft X-ray laser facilities were invited (see program in Appendix). There was a very strong response within the community with 139 registered participants and totally 129 people attending the workshop. What is remarkable for a workshop of this type is that 100 registered scientists were from Sweden from all major universities (see Appendix for list of participants) demonstrating a strong interest for SXL in Sweden.

The workshop consisted of plenary talks representing new accelerator science from LCLS and FERMI, ultrafast pump opportunities based on development at the Lund Laser Centre and the Stockholm-Uppsala FEL centre, the capabilities and soft X-ray scientific programs at LCLS-II, FERMI, European XFEL, FLASH and Swiss FEL. There were 3 parallel sessions with scientific talks representing atomic, molecular and optical (AMO) physics, chemistry (CHEM), condensed matter physics (COND) and life science (LIFE). Almost half of the time of the workshop was devoted to break-out groups in AMO, CHEM, COND, LIFE and as well FEL science to discuss the science case and the characteristics that should be unique for SXL representing the Swedish scientific community. This report is the outcome of this workshop, based on contributions from its participants, and presents the science case for SXL at MAX IV.



*Figure 1.2. Pictures from the workshop.*

## 2. Short Outline of the SXL Beamline

---

- *The baseline design of the SXL will deliver coherent, ultrashort, soft X-ray pulses with full polarization control.*
- *A broad range of pump-possibilities for pump-probe experiments is scheduled from day one.*
- *Two-pulse and two-color options will be developed at an early stage.*
- *Seeding schemes and attosecond pulses are envisioned at a second stage.*
- *The existing MAX IV linac is well prepared to serve the SXL, and space is available.*

The advancement of bright coherent photon sources in the soft X-ray regime is being strongly pursued. Both laser-based and electron accelerator-based techniques are being explored. In the photon energy range above 0.25 keV (5 nm) the most powerful sources at hand are electron accelerator-based, the free electron laser (FEL).

The SXL beamline will take light from a FEL source which utilizes a high energy electron beam passing down an undulator as amplifier. The free electrons in such a beam do in principle not have any limitations as to the photon energy produced and can thus act as amplifiers also in the X-ray region, where traditional lasers are less developed. In this region the main sources are synchrotrons, such as MAX IV. While those sources have very strong benefits, they are not well suited to produce extremely short pulses at very high peak intensities and they are not longitudinally coherent. The coherence can be gained by filtering the radiation, but this will reduce intensity dramatically. The laser sources based on high-order harmonic generation (HHG) [2.1] perform well at photon energies below 0.1 keV, but still need development to reach photon energies above 0.25 keV.

The FEL sources on the other hand can provide exactly this: short pulses, high power and coherence. They are also capable of generating two color and double pulses. For the applications described in this report these are fundamental

performances, which cannot be provided today at any other kind of photon source.

The SXL beamline at MAX IV will provide high power pulses, with pulse lengths below 100 fs in the 0.25-1 keV photon energy range. These pulses can optionally also contain two colors, double pulses with tunable delay, helical polarization and in a later stage seeding for full control of the optical mode. The key to achieving these performances is the MAX IV 3 GeV injector [2.2], which already today delivers to the SPF (Short Pulse Facility) a compressed electron bunch at 3 GeV suitable for the operation of the FemtoMAX beamline [2.3] and the future SXL.

### 2.1 The MAX IV facility as SXL driver

The MAX IV facility was prepared to act as a driver for a free electron laser already from the design phase which started around year 2000. This ability is already exploited by the SPF with its first beamline, FemtoMAX. Technically a photo cathode RF gun controlled by a Titanium:Sapphire (Ti:Sa) laser system delivers high brightness electron pulses to the linear accelerator (fig. 2.1). These pulses are compressed in two bunch compressors built to be self-linearizing and retaining the low emittance from the source. These pulses are delivered to the FemtoMAX in the SPF where incoherent X-ray pulses up to 20 keV are generated. The final

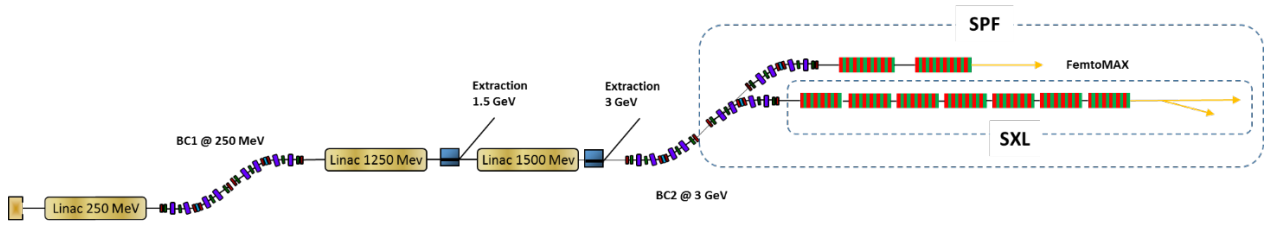


*Figure 2.1. The SXL in the SPF and the MAX IV linear accelerator.*

energy today of the MAX IV injector is 3 GeV which is very well matched for driving a FEL in the desired photon energy range 0.25-1 keV (1-5 nm).

## 2.2 Tentative performance of the SXL

The SXL concept is shown in Table 2.1 where orders of magnitude of the most relevant

parameters for the photon pulses generated in the SXL are given. Furthermore, fig. 2.2 displays the photon pulse characteristics in more detail for self-amplified spontaneous emission (SASE) and self-seeded modes. These simulations of the system (from electron gun to radiation in the undulators) show that there is potential for very high performance but also visualize the potential benefits of seeding the system.

*Table 2.1. A set of tentative parameters for the SXL (Assuming a planar in-vacuum undulator with 18 mm period. Values given by analytical approximation.)*

Wavelength	1 nm	5 nm
Photon energy	1 keV	0.25 keV
e-Energy	3 GeV	1.5 GeV
Undulator type	In-vacuum	
Period	18 mm	
K	2.51	2.7
L-saturation	18 m	12 m
Photon power (peak)	(GW)	(GW)
Flux (peak)	$(10^{24})$	$(10^{25})$ ph/s*BW
Brilliance (peak)	$(10^{31})$	$(10^{30})$ ph/s*BW*mm <sup>2</sup>
Photons/pulse	$(10^{12})$	$(10^{12})$
Pulse length (RMS)	10 fs	10 fs

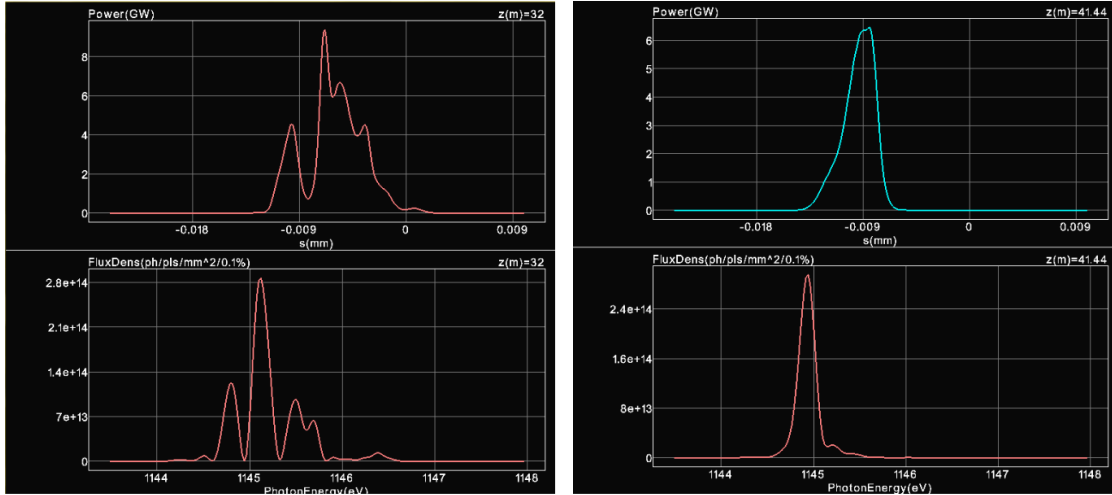


**Figure 2.2.** Photon pulse initial simulation results. **Top:** Longitudinal power profile. **Bottom:** Spectrum. **Left:** SASE. **Right:** Self-seeded. (Simulations following the electron pulse from the cathode to the FEL by use of the codes ASTRA, elegant and Genesis 1.3.)

## 2.3 Some possible features of the SXL on MAX IV

The SXL will not only be a very powerful photon source, but it will also provide experimental facilities not present elsewhere. These include integration to the FemtoMAX beamline, the beamlines and user facilities at the MAX IV 3 and 1.5 GeV rings, pump sources and the research environment around the Lund Laser Centre. Synchronization schemes, diagnostics and pump-probe schemes are being developed for the facilities in operation and will be fully available for the SXL from day one.

In these early times of the design of the SXL itself there are still many options that can be explored. A fundamental issue for the performance and the overall considerations for the SXL is the choice of undulators (see below). The SXL will early in the development integrate both two color and two pulse operation. A multiple set of pump sources will be made available and the SXL is intended to be flexible such that seeding schemes and ultrashort pulse operation modes can be implemented in a second phase.

### Undulators – Full polarization control

So far studies have been made based on in-vacuum undulators with relatively short period. These are compact devices but cannot generate helical radiation. The required operation energy range of the accelerator is also fairly large and thus alternative solutions should be studied.

Due to the flexibility and energy of the linac driver the SXL may be built around a choice of undulator types: short period in-vacuum devices (18 mm period), standard out-of-vacuum undulators (25 mm period), APPLE II helical undulators (30-35 mm period) and also using the APPLE III concepts currently being developed with the Delta undulators aimed for LCLS-II [2.4] and the adaptation made for SwissFEL [2.5] of these devices. Especially the options where the wavelength range 1-5 nm can be covered by one single electron-beam energy will provide easy co-operation with the storage rings at MAX IV.

### Two colors, two pulses

The most straightforward method to achieve two colors and two pulses is by split undulators. A first undulator chain brings the system close to saturation at one photon wavelength. A chicane erases the generated microbunching and provides

a suitable delay for the second pulse, which is generated in a following undulator chain. This kind of system provides flexibility, not only for the two pulse generation, but also to work on schemes developing the facility in the future (read: ultrashort pulses, tapering, seeding and harmonic operation). The disadvantage is that a longer undulator chain is needed.

Other techniques involve either accelerating two pulses from the RF gun or splitting the electron pulse in two pulses with slightly different energies. Both these methods are more demanding and less flexible when it comes to accelerator operation, while they may provide a more compact system.

### **Synchronization**

Synchronization of a SASE FEL is difficult as the inherent jitter in the SASE process is normally bigger than the pulse lengths achieved. Different methods are being developed at the SPF for the FemtoMAX beamline already today which include generation of terahertz (THz) pulses from the very same electron pulse as produced the X-ray photons. This is more or less the only way to achieve synchronization around 10 fs. Fully external pumping systems rely on synchronization to the RF systems and the gun laser systems and can thus not achieve a better synchronization.

### **Pump-probe**

Pump-probe methods are becoming increasingly important and are also one of the key demands from the users as explained in the scientific motivations. Laser pumps in the visible and vacuum ultraviolet (VUV) range are already today operational at the FemtoMAX beamline and the technology will be directly transferred to SXL. THz pump sources are equally important and a THz synchronization pulse line is already being constructed in the SPF. The implementation of more powerful THz pumps is described in Chapter 3.

Soft X-ray pump sources rely on HHG lasers, which is part of the Lund Laser Centre (LLC) development program. These advances will be brought into the SXL to provide a full range of pump sources from THz to soft X-rays.

### **Ultrashort pulses**

The generation of ultrashort pulses (single femtosecond and attosecond) is a field under development. While several concepts such as Slotted foil [2.6], slicing, single spike and mode-locking and some proof-of-principle work [2.7] is at hand this will be a field of development for the SXL. It is in this context important to have a flexible and modular design of the undulator chain, to allow different concepts to be explored.

### **Seeding**

Seeding in the 0.25-1 keV photon energy range is at the moment only demonstrated with self-seeding schemes, where the electron beam creates an amplified photon beam which is passed through a monochromator and re-injected onto the electron beam, which then restarts the amplification process at the selected optical mode [2.8]. This method results in almost full coherence, but retains a rather large intensity jitter.

Better mode locking can be made by using an external source for seeding. This can be done at the actual wavelength of interest using a HHG laser. These sources do not at the moment reach below 5 nm with powers enough to provide seeding, though the development is strong and the SXL will develop towards laser seeding in collaboration with the LLC. Another method is external seeding at longer wavelengths and harmonics created by the electron beam itself. Methods like High Gain Harmonic Generation (HG), cascade or Echo-Enabled Harmonic Generation (EEHG) are being developed at longer wavelengths and may reach below 5 nm following further development.

As the users at the moment do not put highest priority to self-seeded systems it is intended to

start the SXL in SASE mode and work to develop external laser seeding in a second stage.

## 2.4 Possible layouts

There are two main alternatives to place the SXL in the SPF. The FemtoMAX beamline in the SPF occupies the second branch line position. Adjacent is the first branch line position in which the SXL can be placed. The second alternative is in the space called “future klystron gallery”, which is slightly longer and also provides more space for the experimental stations.

Flexibility and modularity are key elements in the future development of the SXL and thus have to be taken into account. A possible way would be to start by one SASE system, expand for two color/two pulse and finally add seeding.

### The SPF 1 beamline location

An easy solution to fit the SXL into the SPF is to use the slot beside the FemtoMAX, slot 1 (fig. 2.3). This solution will interfere the least with the accelerator operation and require the smallest adaptations of the building. On the other

hand this solution allows only for a rather short SXL system with a basic SASE FEL operation and a short limiting distance to the first mirror in the beamline. In this location the SXL will have approximately 50 m available for the FEL itself (including electron matching section, undulators and diagnostics). The beamline and experimental station can then be placed in a similar location as the FemtoMAX.

### “The Future klystron gallery”

A second solution is to construct the SXL in the tunnel called “the future klystron gallery” (fig. 2.4). Here the available length for the undulator section and the space for the beamline is larger. This will provide some flexibility and a more relaxed design. The interference with the accelerator operation under installation is bigger and the requirements for rebuilding are also larger. This can be done in two steps though where a basic SASE system is installed and put into operation, and then upgraded to a longer undulator system. Though space is larger a careful study has to be made on which features of the SXL that can be realized and where compromises are needed.

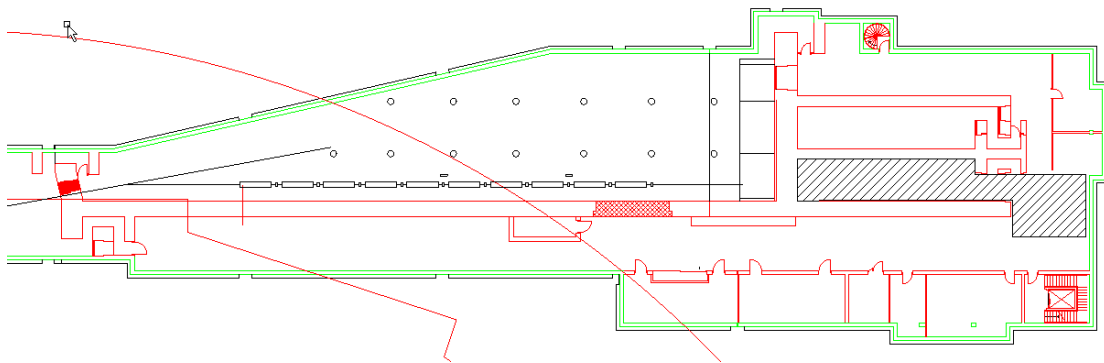


**Figure 2.3.** Installation in Slot 1 of the SPF. Hatched area is available for the beamline and experimental station.

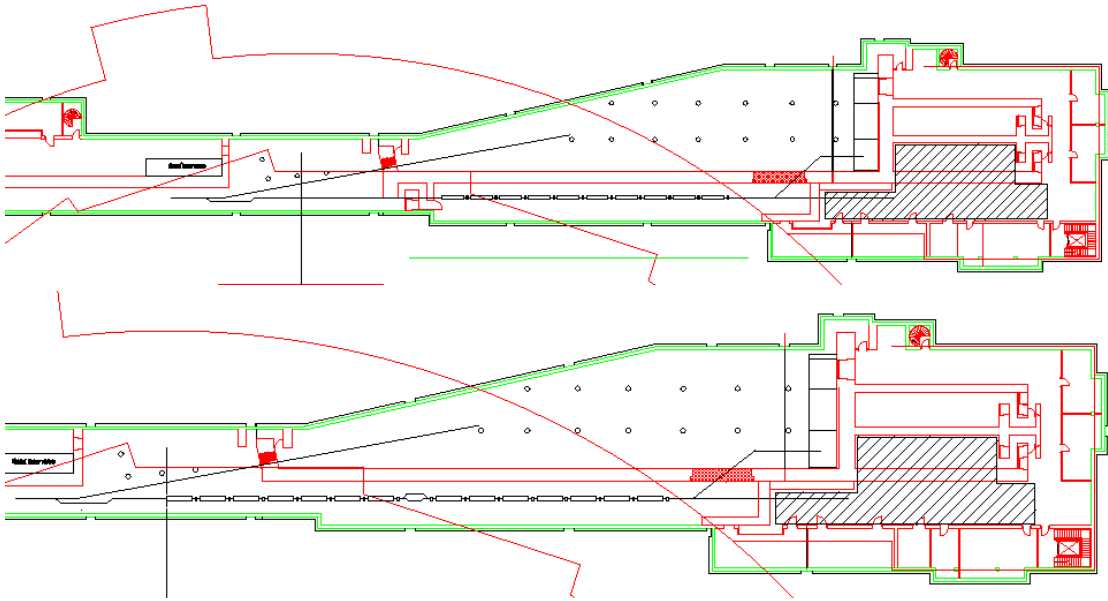


**Figure 2.4.** Installation in the “future klystron gallery”. **Top:** First basic SASE system. **Bottom:** An extended more flexible system. Hatched area available for the beamline and experimental station.

## References

- [2.1] Lewenstein, M., Balcou, P., Ivanov, M. Y., L’Huillier, A. & Corkum, P. B. “Theory of high-harmonic generation by low-frequency laser fields.” *Phys. Rev. A* **49**, 2117–2132 (1994).
- [2.2] Thorin, S., Andersson, J, Curbis, F., Eriksson, M., Karlberg, O., Kumbaro, D., Mansten, E., Olsson, D., Werin, S. “The MAX IV Linac” *Proceedings, 27th Linear Accelerator Conference, LINAC2014 : Geneva, Switzerland, August 31-September 5*, (2014).
- [2.3] Werin, S., Thorin, S., Eriksson, M. & Larsson, J. “Short pulse facility for MAX-lab.” *Nucl. Instruments Methods Phys. Res. Sect. A Accel. Spectrometers, Detect. Assoc. Equip.* **601**, 98–107 (2009).
- [2.4] Nuhn, H-D. “DELTA undulator LCLS” *slac-pub-15743, Presented to the 35rd International Free Electron Laser Conference (FEL 2013) New York, NY, August 25-29*, (2013).
- [2.5] Schmidt, Th. “APPLE III undulator of DELTA type for SwissFEL” *Proceedings of FEL2014, Basel, Switzerland (2014)*.
- [2.6] Emma, P. *et al.*, “Attosecond X-ray pulses in the LCLS using the slotted foil method” *Proceedings of the 2004 FEL Conference*, 333-338 (2004).
- [2.7] Ding, Y. “Generation of femtosecond to sub-femtosecond x-ray pulses in free-electron lasers.” *Proc. SPIE 9512 Advances in X-ray Free-Electron Lasers Instrumentation III, 95121B* (May 12, 2015).
- [2.8] Ratner, D. *et al.* “Experimental Demonstration of a Soft X-Ray Self-Seeded Free-Electron Laser.” *Phys. Rev. Lett.* **114**, 54801 (2015).

# 3. Unique Characteristics of SXL

---

Three unique properties of the SXL will be complementary to present FEL facilities:

- *A spectrally broad pumping range with potential for attosecond temporal resolution and strong single-cycle THz pulses.*
- *Unique detection schemes using nonlinear effects to enhance the cross section for resonant inelastic X-ray scattering (RIXS).*
- *An imaging capacity that, through the synergies with other beamlines at MAX IV, creates a unique platform for imaging in the fields of life science and condensed matter.*

## 3.1 Bridging the spectral gap – a broadband sub-fs pump facility

Studies of femtosecond dynamics, often referred to as “ultrafast” and made possible by the commercial availability of Ti:Sa lasers, have revolutionized many realms of science. For instance, the demonstration of femtochemistry techniques at the end of the previous century [3.1] marked a starting point for scientists from a wide variety of fields to envisage the possibility of following and controlling complex molecular structural dynamics in time. Examples of such ultrafast dynamics, of fundamental importance for our understanding of chemical processes

around us, are fragmentation, isomerization, proton transfer and the dynamics around conical intersections. By using one pulse to start the dynamics (pump) and another, time-delayed, pulse to take a snapshot of the molecule (probe), a “molecular movie” can be recorded by taking a sequence of snapshots of the molecular structure for different delays between the pump and probe pulses. Similar pump-probe experiments have been conducted within condensed matter physics. Here, the goal is to understand non-equilibrium dynamics that can lead to the creation of transient states of matter that are not allowed in thermodynamic equilibrium. In turn, this may allow for the control of the properties of matter at timescales that are orders of magnitude faster than what nowadays is achievable.

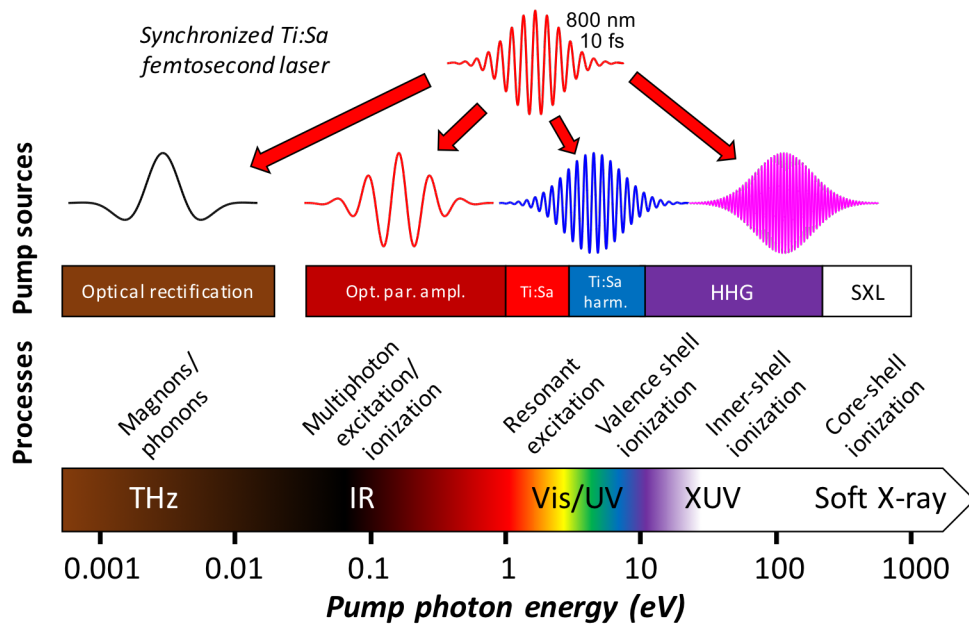


**Figure 3.1.** Overview of the envisaged pump spectral range at SXL. **Top:** Available pump sources derived from the synchronized Ti:Sa femtosecond laser. **Bottom:** The spectral range that will be covered at SXL with examples of the relevant processes accessible using different pump photon energies.

All these experiments have traditionally been performed using probe pulses in the infrared (IR), visible (Vis) and ultraviolet (UV) regimes, but the most recent addition to the ultrafast toolbox are the X-ray FELs [3.2]. At these facilities, in addition to X-ray/X-ray pump/probe experiments performed either through splitting the X-ray FEL pulses or by operating the FEL in a multi-pulse mode, the use of external synchronized laser systems makes it possible to pump a variety of dynamics that can then be probed using the FEL pulses. Ever since the opening of the world's first extreme ultraviolet (XUV) FEL, FLASH, as a user facility in 2005 the number of users requesting the external pump-probe laser has steadily increased and today more than half of the accepted proposals make use of the external laser. At FERMI, similar figures apply and at LCLS over 70% of the experiments use the external laser. In fact, one could go as far as to say that one of the keys to the tremendous success of LCLS is the availability and quality of the external pump laser, and it is clear that a *well-working laser infrastructure*, a *thought-through laser-beamline integration* and a *highly skilled and dedicated laser team* are keys to successful

laser/FEL experiments. Further, in addition to using a synchronized femtosecond Ti:Sa-laser with wavelength around 800 nm (1.55 eV photon energy) as a pump source in FEL experiments, one might use various frequency conversion techniques to access a much wider spectral region, as illustrated in the top panel of fig. 3.1. Depending on the photon energy of the pump pulse, very different dynamics can be triggered, as indicated in the bottom panel of fig. 3.1. To date, the spectral region covered by the pump sources at the different FELs around the world varies, but at no existing FEL is it possible to get access to the full spectral region shown in fig. 3.1, and at no FEL today is it possible to use pump pulses in the important VUV and XUV regions, where the process of high-order harmonic generation (HHG) even allows for the production of pulses with attosecond duration.

SXL will, from the start, be equipped with a broadband sub-femtosecond pump facility, covering photon energies from 1 meV using optical rectification up to the photon energies accessible from the FEL itself using HHG. This will make SXL a unique facility and, in addition,

by using HHG for achieving the unique coverage of the XUV spectral region one allows for ultimately breaking the femtosecond barrier in future pump-probe experiments. These features will be made possible through paying careful attention to the three “keys to successful laser/FEL experiments” presented above already in the planning phase, and through the synergies expected from the close collaboration with the expertise available at the Lund Laser Centre. While the IR, Vis and UV spectral regions are straightforward to cover through the use of optical parametric amplification (OPA), the Ti:Sa fundamental and frequency doubling/tripling of the Ti:Sa pulses, respectively, we briefly describe below the techniques that will be used to access the THz and XUV spectral regions.

### The THz pump source

Broadband THz radiation can be generated from a femtosecond laser system via an optical rectification process that occurs in nonlinear crystals with finite second-order susceptibility [3.3]. The electric and magnetic fields exiting the crystal after such process have the shape of a single-cycle transient, with a sharp peak of sub-picosecond duration. At present, the largest peak electric (magnetic) fields are of the order of 100 MV/m (0.3 T). Those are typically achieved using LiNbO<sub>3</sub> crystals pumped with Ti:Sa lasers [3.4], alternatively using organic crystals [3.5] pumped with mid-IR radiation generated via optical parametric amplification. The THz fields generated have bandwidth in the 0.1–4 THz region, with the upper limit being imposed by phonon absorption that is intrinsically present in solid crystals.

Single-cycle THz fields are extremely interesting for condensed matter physics, because they allow for time-resolved experiments where the dynamics are driven by low-energy excitations, where work is done on the system, rather than entropy being dumped into the material. In general, THz experiments can be divided into two types, resonant and non-resonant:

- (i) *Resonant experiments.* In this case, one aims at driving a resonant excitation within the bandwidth of the THz pulse. Examples in this regard are the excitation of antiferromagnetic modes in NiO [3.6], of nonlinear phonon dynamics in superconductors [3.7] or electromagnons [3.8].
- (ii) *Non-resonant experiments.* Here, the goal is to use the large *peak* electric or magnetic field that is present in a broadband signal. Examples in this case are THz-induced metal-insulator transitions [3.9] or ultrafast magnetization dynamics [3.10]. Very recently, it has also been shown that strong THz fields can also be used as an additional degree of freedom to control a catalytic reaction [3.11].

Despite these achievements, we are still at the dawn of experiments that combine THz radiation and X-rays. There is a large interest within the research community for an easier access to THz sources, in particular if combined with X-ray probing capabilities. A reliable operation of a laser-based THz source is therefore considered crucial for a successful user operation of the SXL facility. In addition, we also envisage schemes for implementing even greater THz capabilities, using accelerator-based sources.

### The HHG pump source

High-order harmonics are generated in the interaction between an intense (typically femtosecond duration) IR laser pulse and a gas [3.12]. They manifest themselves as a broad spectrum of peaks corresponding to odd harmonics of the driving laser frequency, reaching up to high photon energies in the XUV region (~100 eV). HHG is generally understood in a simple semi-classical model in which the intense IR laser field is used to tunnel ionize the target, creating a free electron which is subsequently accelerated by the strong field of the laser. For some ionization times within the laser cycle, the electron can be driven back to the ion with high kinetic energy and re-collide. Upon re-collision, the electron can recombine with its

parent ion under the emission of broadband XUV radiation with attosecond duration. Since the process takes place once for every half-cycle of the driving laser field, distinct harmonic peaks appear as a result of the repetition of the emission process, and in the temporal domain the result is an attosecond pulse train (APT), first measured experimentally in 2001 [3.13]. The HHG source that will be implemented at SXL can be used in two different modes, depending on the dynamics that one wants to study:

- (i) *Femtosecond experiments.* By isolating a single harmonic peak using a time-compensated monochromator [3.14], femtosecond pulses in the XUV regime are obtained, which can be used to study single-photon ionization and excitation-induced dynamics such as molecular fragmentation and isomerization as well as auto-ionization dynamics.
- (ii) *Attosecond experiments.* By *e.g.* phase-stabilization of the driving laser (*i.e.* locking the phase of the electric field of the laser pulse to the position of the intensity envelope) and/or modulation of the polarization state of the driving pulse by optical schemes one can isolate a single attosecond pulse out of the generated APT [3.15]. With such attosecond pulses in combination with a future attosecond pulse duration of SXL, one will be able to initiate and probe charge dynamics such as ultrafast charge migration following prompt ionization of molecules, proton migration, post Born-Oppenheimer dynamics around conical intersections as well as to attempt observing fundamental quantum transport in condensed matter, such as Bloch oscillations.

A crucial parameter for pump-probe experiments using a pump pulse derived from an external laser is the stability of the delay between the external laser and the SXL. With state-of-the-art synchronization techniques the jitter between the two sources will be on the order of 10 fs [3.16], which will be sufficient for most

experiments. However, in experiments where a better resolution is required (*e.g.* for the attosecond experiments described above), the delay between the pump and the probe pulse will be measured on a single shot basis so that the acquired single-shot data can be sorted in the post-analysis [3.17]. The implementation of such measurements can for example make use of so-called photoelectron streaking, which is a well-established technique within the attosecond physics community [3.18].

### 3.2 Unique detection schemes

Energy resolution in conventional soft X-ray spectroscopy is often compromised by the need for high throughput. Typically, the angular distribution of the emission is quasi-isotropic and reasonably sized gratings, mounted in grazing incidence, can collect only a small fraction. In addition, a large source size requires a micron-sized input slit, at some distance away from the source. Hence, the fraction of the emission, which can be analyzed, is generally around  $10^{-5}$ .

The situation is completely different for analysis of stimulated RIXS (SRIXS) (fig. 3.2). As the emittance of the FEL beam is diffraction limited, ambitious emittance-preserving optics must be designed to focus the beam to a small spot in the interaction region. A sub-micron focus of the primary beam is required to attain sufficient intensity for nonlinear X-ray physics, and as the angular distribution of the stimulated emission is the same as the primary radiation, X-ray spectroscopy is faced with a situation of having a low-emittance source of secondary photons to analyze. Collection efficiency is no longer an issue, and instruments can be optimized for ultimate energy resolution. The width of the spectral features will be determined by the pulse duration and the fundamental Heisenberg uncertainty principle. In the case of transient X-ray absorption with short-duration broad-band probe pulses the limit will be set by the intrinsic

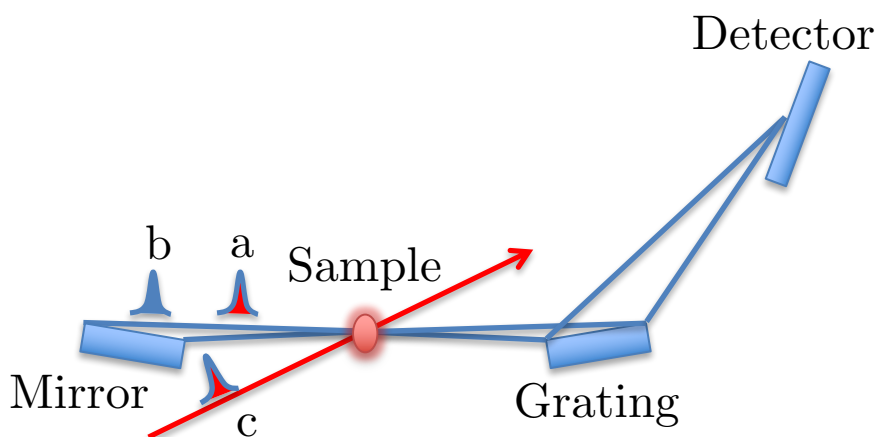


**Figure 3.2.** Schematic setup for stimulated RIXS and transient absorption. Impulsive RIXS requires only one broad-band FEL pulse (a). Ambitious refocusing is required to attain sufficient intensity for nonlinear processes and facilitate spectroscopy of the emitted radiation. All X-ray pump-probe experiments are feasible with a delayed probe pulse (b) of slightly different color. Transient X-ray absorption spectroscopy using a synchronized laser pump (c) and a broad-band FEL probe pulse can be pursued in the same setup.

natural width of the final states, which may very well be smaller than the pulse width.

### 3.3 Imaging for life science and condensed matter

The exceptionally low emittance below 0.3 nm rad and resulting coherence properties of the X-ray beam of MAX IV's 3 GeV ring makes it ideal for nanoscale imaging of molecules and materials in condensed matter and life science that cannot be studied using X-ray crystallography. Thus, several MAX IV beamlines of the initial seven that have been funded will focus on various types of X-ray

imaging. NanoMAX [3.19] is a hard X-ray nanoprobe beamline with a target energy range of 5-15 keV for scanning transmission X-ray microscopy (STXM) and coherent diffractive imaging methods when using a 10 nm spot size focused with Fresnel zone plates. SoftiMAX [3.20] focuses on STXM and coherent lensless X-ray imaging [3.21] in an energy range of 250-2500 eV with full polarization control up to 1700 eV. STXM will have a dedicated experimental station with a target resolution of 10-15 nm, whereas the coherent X-ray imaging station will have a modular setup where X-ray optics, sample environments and detectors can be exchanged for holography, ptychography and coherent diffractive imaging.

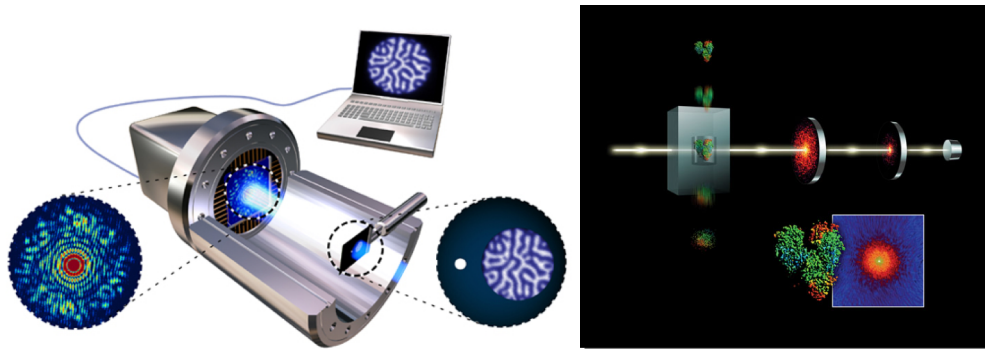


**Figure 3.3. Left:** Lensless holographic imaging of magnetic nanostructures. Monochromatic, coherent, circularly polarized X-rays illuminate a mask-sample structure. Two apertures in this mask define the object and reference beam, and the resulting hologram is recorded on a charge-coupled device (CCD) detector. A single 2-dimensional (2D) Fourier transformation yields an image of the object. (Reprinted by permission from J. Stöhr, SLAC National Accelerator Laboratory. Image rendered by Michael Hyde.) **Right:** Coherent diffractive imaging used to determine the atomic structure of a complicated biomolecule. Single biomolecules of e.g. a protein in its native state are injected into vacuum in a particle beam using an aerosol injector. The particle beam is intersected by the ultrashort and ultrabright X-ray pulses produced by a free electron laser, which produce a series of coherent diffraction patterns of the randomly oriented biomolecules on two CCD detectors before they disintegrate due to Coulomb explosion. The ensemble of diffraction patterns can be oriented into a 3-dimensional (3D) diffraction volume using Bayesian methods, which in turn can yield a 3D image of the electron density of the biomolecule through iterative phase retrieval algorithms. (Reprinted by permission from SLAC National Accelerator Laboratory.)

The SXL beamline extends nanoscale imaging at MAX IV to ultrafast processes and higher radiation dose through diffraction before destruction [3.22], making it possible to record time-resolved movies of molecules and materials at nanometer resolution (see fig. 3.3). Lensless holographic imaging [3.23] can be applied to magnetic nanostructures [3.24] using circularly polarized X-rays (see fig. 3.3, left). Coherent diffractive imaging is feasible at X-ray free electron lasers to study viruses [3.25, 3.26], living cells [3.27] and cell organelles [3.28] (see fig. 3.3, right) since the resolution limit set by

radiation damage can be circumvented through diffraction before destruction [3.22]. The possibility of being able to perform static measurements at SoftiMAX or NanoMAX and time-resolved studies of the same sample at the SXL beamline in the same building makes it possible to share algorithms, experimental setups, and expertise in a way not possible at other free electron lasers. The synergy between the SXL beamline and the nanoscale imaging beamlines at MAX IV's 3 GeV ring and the wide range of X-ray imaging techniques they cover is a unique capability only present at the MAX IV facility.

## References

- [3.1] Zewail, A. H. “Femtochemistry: Atomic-Scale Dynamics of the Chemical Bond.” *J. Phys. Chem. A* **104**, 5660–5694 (2000).
- [3.2] Feldhaus, J., Arthur, J. & Hastings, J. B. “X-ray free-electron lasers.” *J. Phys. B At. Mol. Opt. Phys.* **38**, S799–S819 (2005).
- [3.3] Rice, A. *et al.* “Terahertz optical rectification from (110) zinc-blende crystals.” *Appl. Phys. Lett.* **64**, 1324 (1994).
- [3.4] Hoffmann, M. C. *et al.* “Intense ultrashort terahertz pulses: generation and applications.” *J. Phys. D. Appl. Phys.* **44**, 83001 (2011).
- [3.5] Hauri, C. P., Ruchert, C., Vicario, C. & Ardana, F. “Strong-field single-cycle THz pulses generated in an organic crystal.” *Appl. Phys. Lett.* **99**, 161116 (2011).
- [3.6] Kampfrath, T. *et al.* “Coherent terahertz control of antiferromagnetic spin waves.” *Nat. Photonics* **5**, 31–34 (2011).
- [3.7] Mankowsky, R. *et al.* “Nonlinear lattice dynamics as a basis for enhanced superconductivity in  $\text{YBa}_2\text{Cu}_3\text{O}_{6.5}$ .” *Nature* **516**, 71–73 (2014).
- [3.8] Kubacka, T. *et al.* “Large-amplitude spin dynamics driven by a THz pulse in resonance with an electromagnon.” *Science* **343**, 1333–6 (2014).
- [3.9] Liu, M. *et al.* “Terahertz-field-induced insulator-to-metal transition in vanadium dioxide metamaterial.” *Nature* **487**, 345–348 (2012).
- [3.10] Vicario, C. *et al.* “Off-resonant magnetization dynamics phase-locked to an intense phase-stable terahertz transient.” *Nat. Photonics* **7**, 720–723 (2013).
- [3.11] LaRue, J. L. *et al.* “THz-Pulse-Induced Selective Catalytic CO Oxidation on Ru.” *Phys. Rev. Lett.* **115**, 36103 (2015).
- [3.12] Ferray, M. *et al.* “Multiple-harmonic conversion of 1064 nm radiation in rare gases.” *J. Phys. B At. Mol. Opt. Phys.* **21**, L31–L35 (1988).
- [3.13] Paul, P. M. *et al.* “Observation of a Train of Attosecond Pulses from High Harmonic Generation.” *Science* **292**, (2001).
- [3.14] Poletto, L. & Villoresi, P. “Time-delay compensated monochromator in the off-plane mount for extreme-ultraviolet ultrashort pulses.” *Appl. Opt.* **45**, 8577 (2006).
- [3.15] Baltuška, A. *et al.* “Attosecond control of electronic processes by intense light fields.” *Nature* **421**, 611–615 (2003).
- [3.16] Schulz, S. *et al.* “Femtosecond all-optical synchronization of an X-ray free-electron laser.” *Nat. Commun.* **6**, 5938 (2015).
- [3.17] Schorb, S. *et al.* “X-ray–optical cross-correlator for gas-phase experiments at the Linac Coherent Light Source free-electron laser.” *Appl. Phys. Lett.* **100**, 121107 (2012).
- [3.18] Itatani, J. *et al.* “Attosecond Streak Camera.” *Phys. Rev. Lett.* **88**, 173903 (2002).
- [3.19] Johansson, U., Vogt, U. & Mikkelsen, A. “NanoMAX: a hard x-ray nanoprobe beamline at MAX IV.” *Proc. SPIE 8851 X-ray Nanoimaging: Instruments and Methods, 88510L* (September 26, 2013).
- [3.20] Cerenius, Y., Hennies, F. & Fernandes Tavares, P. “Status of the MAX IV Laboratory.” *Synchrotron Radiat. News* **29**, 34–38 (2016).
- [3.21] Chapman, H. N. & Nugent, K. A. “Coherent lensless X-ray imaging.” *Nat. Photonics* **4**, 833–839 (2010).
- [3.22] Chapman, H. N. *et al.* “Femtosecond diffractive imaging with a soft-X-ray free-electron laser.” *Nat. Phys.* **2**, 839–843 (2006).

- [3.23] Eisebitt, S. *et al.* “Lensless imaging of magnetic nanostructures by X-ray spectroholography.” *Nature* **432**, 885–888 (2004).
- [3.24] Wang, T. *et al.* “Femtosecond Single-Shot Imaging of Nanoscale Ferromagnetic Order in Co / Pd Multilayers Using Resonant X-Ray Holography.” *Phys. Rev. Lett.* **108**, 267403 (2012).
- [3.25] Seibert, M. M. *et al.* “Single mimivirus particles intercepted and imaged with an X-ray laser.” *Nature* **470**, 78–81 (2011).
- [3.26] Ekeberg, T. *et al.* “Three-Dimensional Reconstruction of the Giant Mimivirus Particle with an X-Ray Free-Electron Laser.” *Phys. Rev. Lett.* **114**, 98102 (2015).
- [3.27] van der Schot, G. *et al.* “Imaging single cells in a beam of live cyanobacteria with an X-ray laser.” *Nat. Commun.* **6**, 5704 (2015).
- [3.28] Hantke, M. F. *et al.* “High-throughput imaging of heterogeneous cell organelles with an X-ray laser.” *Nat. Photonics* **8**, 943–949 (2014).

# 4. AMO Science

## 4.1 Ultrafast charge and structural dynamics

- *How are chemical properties and reactions brought about by the ultrafast dynamical interaction between electrons and nuclei?*
- *Can we produce the ultimate Heisenberg limited molecular movie?*
- *Can we see the details of a molecular explosion?*

The ultrafast transfer of charge in a molecule is a fundamental process in nature, playing a crucial role in several chemical, biological and physical processes. Examples for these are photosynthesis, where an electronic event acts as the trigger of a chemical change, and charge transfer through DNA, important for *e.g.* mutation and development of cancer. Although both theoretical and experimental research have made substantial progress in the last decades a

wealth of unanswered questions remain concerning charge transfer in molecules as well as the associated structural changes.

The challenge in obtaining the complete picture of a photoinduced chemical reaction is to experimentally access, simultaneously, the different timescales involved. The photon, starting the process, is absorbed by the electrons of the molecule, initiating electron dynamics typically taking place on the attosecond timescale, as exemplified in fig. 4.1. The electron dynamics lead to a rapid change of the electronic potential energy surface of the molecule. The considerably heavier nuclei in the molecule, which move in this potential landscape, are however unable to follow the rapidly changing potential, and rather adapt to the average potential on a femtosecond or even picosecond timescale, and recent theoretical work predict a complicated interplay between the charge and structural dynamics [4.2], calling for experimental imaging approaches that enable access to both timescales

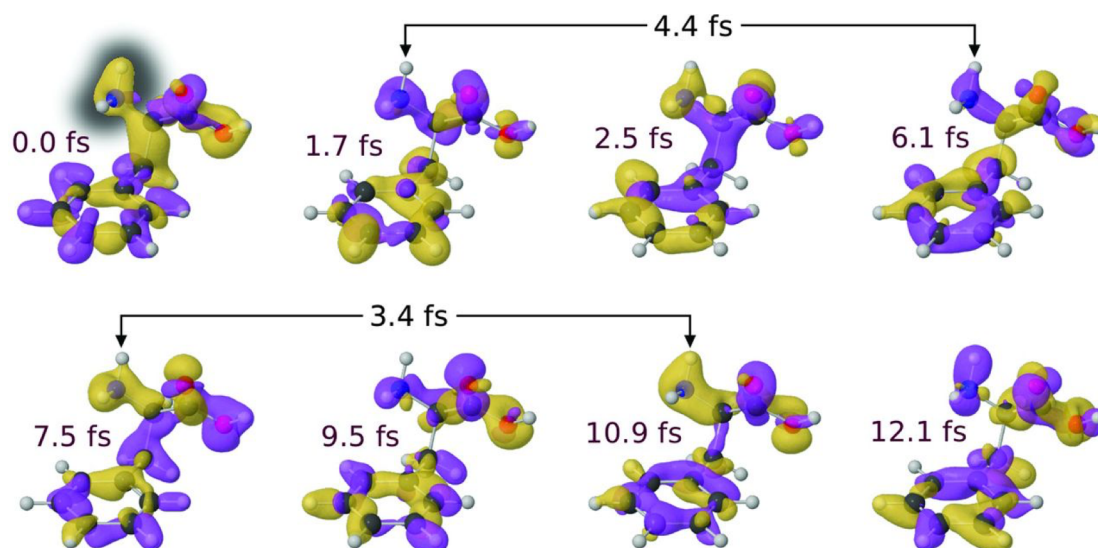


**Figure 4.1.** Snapshots of hole dynamics in the amino acid phenylalanine following ionization by a sub-300-attosecond extreme ultraviolet pulse. The hole density is displayed in yellow and purple, representing the positive and negative hole-density, respectively, with respect to the time-averaged value. [4.1] (Reprinted by permission from AAAS. Calegari, F. et al., *Science* **346**, 336 (2014), copyright (2014).)

during one experiment. Another major challenge is that in order to be able to extract structural information from such experiments, the spatial resolution has to be on the order of the molecular bond length, typically 1 Ångström.

These challenges can be addressed using the unique combination of probe pulses from SXL with femtosecond or ultimately attosecond pulse duration, and VUV or XUV pump pulses with attosecond duration produced through high-order harmonic generation [4.3] at the envisaged broadband pump facility. While the pulse durations will provide the required temporal resolution for structural dynamics (femtosecond) or charge dynamics (attosecond), the short wavelength of the SXL probe pulse will enable a spatial resolution on the order of the length of a typical molecular bond, through *e.g.* photoelectron diffraction following site-specific ionization of the inner electrons of the constituent atoms. The versatility of the envisaged pump source will enable triggering a multitude of different processes, from ionization-induced charge migration in molecules [4.1, 4.4, 4.5] to resonant excitation of plasmons in *e.g.* fullerenes [4.6].

The ability to create molecular movies in which the electronic and nuclear dynamics can be followed in chemical reactions has implications not only for fundamental AMO physics, where attention initially will be given to behavior at conical intersections, and isomerization reactions. This will also be important for applications *e.g.*, in catalysis, battery, and solar cell research, where an atomic-scale understanding is prerequisite for substantial advances.

The dynamics following exposure to short intense X-ray pulses in large molecular systems is of paramount importance for the “diffraction-before-destruction” technique [4.7]. The energy dissipation is complex, and leads eventually to Coulomb explosion in which the multiply charged system breaks into multiple fragments. Using advanced pump-probe schemes and multi-

coincidence measurement methods we aim at attaining vital information about this process, of vital importance for molecular biology. For multi-coincidence measurements efficient electron spectrometers such as magnetic bottles, which also allow for studying ions in a correlated fashion [4.8], will be exploited.

## 4.2 Nonlinear X-ray AMO

- *How will the nonlinear X-ray world change our view on light-matter interactions?*
- *Can we use nonlinear X-ray phenomena to control electron dynamics?*
- *Can the fascinating phenomena, predicted by fundamental theory be exploited in novel methods for materials science?*

Since the advent of the laser, investigation of nonlinear phenomena has changed the view on interaction between light and matter in a profound way. It has led to new spectroscopic techniques such as four-wave mixing, transient grating, and coherent anti-stokes Raman spectroscopy, and to a multitude of methods based on high-harmonic generation. The new concepts are typically developed in AMO physics. The relative simplicity of small quantum systems allows for rigorous tests of fundamental theory, and the acquired understanding is prerequisite for efficient application of the methods on technically relevant processes like catalysis and electrochemistry.

The new X-ray/XUV FEL sources open a pathway to transfer nonlinear spectroscopic techniques to the X-ray domain. Combining the merits of X-ray spectroscopy, especially the ability to gain information about interactions on the atomic time and length scales, with the opportunities given by nonlinear techniques, promises a paradigm shift in the way we look at materials and chemical processes. A wealth of

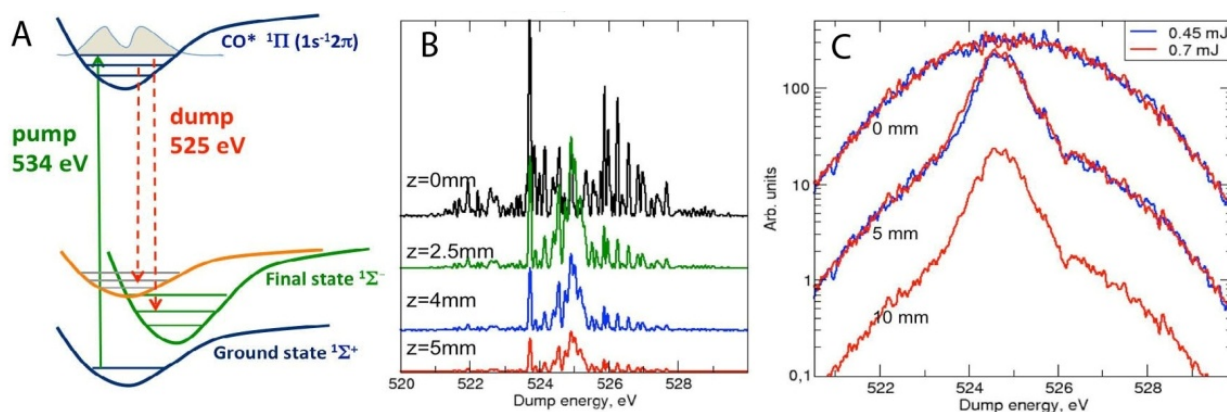


**Figure 4.2.** Theoretical simulations for SRIXS of gasphase CO in X-ray two color mode [4.14]. The broadband XFEL pump pulse creates vibrational population in the core-excited state, while the dump pulse simultaneously stimulates emission on transitions to valence excited states in the CO molecule (A). Propagation of the typical stochastic pulse is illustrated in panel B, where  $z$  is the propagation length: the signal is amplified around the transition to the lowest final state (524.5 eV). (C) SRIXS spectra averaged over an ensemble of 100 individual SASE shots (a typical experimental situation). (Figure 4.2 reprinted by permission from V. Kimberg, KTH.)

novel nonlinear phenomena is predicted [4.9-4.14] (exemplified by stimulated RIXS (SRIXS) in fig. 4.2), and already stimulated impulsive resonant inelastic X-ray scattering [4.15, 4.16], and non-sequential multiphoton resonant absorption has been observed [4.17]. This new field of multi-dimensional nonlinear X-ray spectroscopy is presently being explored experimentally [4.18].

Schemes where all X-ray pump-probe techniques are based on coherent stimulated electronic X-ray Raman scattering are particularly attractive for chemical applications: Impulsive stimulated Raman scattering creates a coherent electronic/vibrational wave packet at the site of atom A in a large molecule, and dynamics are

subsequently probed at the site of atom B by a second X-ray pulse. The probe technique can be based *e.g.* on transient absorption or on a second impulsive X-ray Raman process.

Strong nonlinear effects in Resonant Auger (RA) have been predicted [4.19, 4.20] (fig. 4.3), but have so far been only little investigated experimentally [4.21]. As a showcase the C  $1s^{-1}\pi^*$  RA spectra of CO were considered, showing field-induced non-adiabatic coupling between electronic, vibrational and rotational degrees of freedom. Thus, also the electronic decay channel will be exploited to realize the vision of controlling the ultrafast dynamics by varying the properties of the exciting radiation.

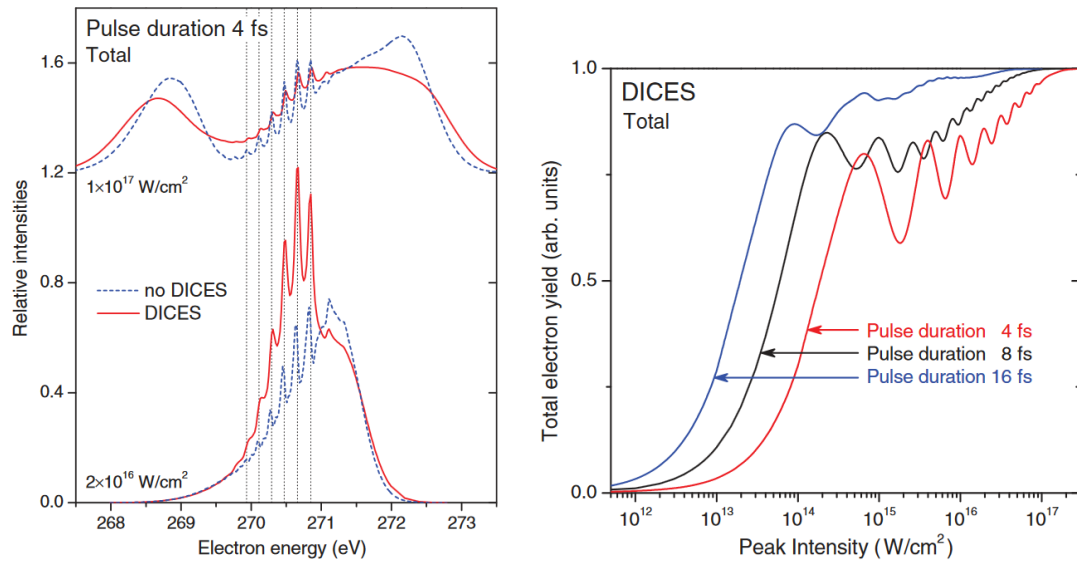


**Figure 4.3. Left:**  $C 1s^{-1}\pi^*$  resonant Auger (RA) spectra of CO ( $A^2\Pi$  state) for two different peak intensities. Doubly Intersecting Complex Energy Surfaces (DICES) as a consequence of the high intensity is predicted to have a large spectral impact; **(right panel)** Total electron yield as a function of peak intensity. (Figure 4.3 reprinted by permission from American Physical Society: P.V. Demekhin et al., *Phys. Rev. A* **84**, 033417 (2011), copyright (2011).)

Predictions of remarkable nonlinear X-ray optical phenomena associated with pulse propagation in dense (ambient pressure) resonant media will be scrutinized experimentally. With the Ar 2p resonance as an example, pulse compression accompanied by self-seeded stimulated resonant Raman scattering, starting from amplified spontaneous emission is predicted

[4.11]. The frequency width of the compressed pulse generates Stokes and anti-Stokes fields caused by four-wave mixing, and the four spectral bands have fine structure caused by the dynamical Stark effect. A slowdown of the pulse up to 78% of the speed of light in vacuum is found because of a large nonlinear refractive index.

## References

- [4.1] Calegari, F. *et al.* “Ultrafast electron dynamics in phenylalanine initiated by attosecond pulses.” *Science* **346**, 336 (2014).
- [4.2] Lünemann, S., Kuleff, A. I. & Cederbaum, L. S. “Ultrafast charge migration in 2-phenylethyl-N,N-dimethylamine.” *Chem. Phys. Lett.* **450**, 232–235 (2008).
- [4.3] Ferray, M. *et al.* “Multiple-harmonic conversion of 1064 nm radiation in rare gases.” *J. Phys. B At. Mol. Opt. Phys.* **21**, L31–L35 (1988).
- [4.4] Cederbaum, L. S. & Zobeley, J. “Ultrafast charge migration by electron correlation.” *Chem. Phys. Lett.* **307**, 205–210 (1999).
- [4.5] Remacle, F. & Levine, R. D. “An electronic time scale in chemistry.” *Proc. Natl. Acad. Sci.* **103**, 6793–6798 (2006).
- [4.6] Scully, S. W. J. *et al.* “Photoexcitation of a Volume Plasmon in C60 Ions.” *Phys. Rev. Lett.* **94**, 65503 (2005).
- [4.7] Neutze, R., Wouts, R., van der Spoel, D., Weckert, E. & Hajdu, J. “Potential for biomolecular imaging with femtosecond X-ray pulses.” *Nature* **406**, 752–757 (2000).
- [4.8] Eland, J. H. D. & Feifel, R. “Double ionisation of ICN and BrCN studied by a new photoelectron–photoion coincidence technique.” *Chem. Phys.* **327**, 85–90 (2006).
- [4.9] Schweigert, I. V. & Mukamel, S. “Probing valence electronic wave-packet dynamics by all x-ray stimulated Raman spectroscopy: A simulation study.” *Phys. Rev. A* **76**, 12504 (2007).
- [4.10] Harbola, U. & Mukamel, S. “Coherent stimulated x-ray Raman spectroscopy: Attosecond extension of resonant inelastic x-ray Raman scattering.” *Phys. Rev. B* **79**, 85108 (2009).
- [4.11] Sun, Y.-P., Liu, J.-C., Wang, C.-K. & Gel’ mukhanov, F. “Propagation of a strong x-ray pulse: Pulse compression, stimulated Raman scattering, amplified spontaneous emission, lasing without inversion, and four-wave mixing.” *Phys. Rev. A* **81**, 13812 (2010).
- [4.12] Biggs, J. D., Zhang, Y., Healion, D. & Mukamel, S. “Two-dimensional stimulated resonance Raman spectroscopy of molecules with broadband x-ray pulses.” *J. Chem. Phys.* **136**, 174117 (2012).
- [4.13] Biggs, J. D. *et al.* “Multidimensional scattering of attosecond x-ray pulses detected by photon-coincidence.” *J. Phys. B At. Mol. Opt. Phys.* **47**, 124037 (2014).
- [4.14] Kimberg, V. & Rohringer, N. “Stochastic stimulated electronic x-ray Raman spectroscopy.” *Struct. Dyn.* **3**, 034101 (2016).
- [4.15] Weninger, C. *et al.* “Stimulated Electronic X-Ray Raman Scattering.” *Phys. Rev. Lett.* **111**, 233902 (2013).
- [4.16] Weninger, C. & Rohringer, N. “Stimulated resonant x-ray Raman scattering with incoherent radiation.” *Phys. Rev. A* **88**, 53421 (2013).
- [4.17] Žitnik, M. *et al.* “High Resolution Multiphoton Spectroscopy by a Tunable Free-Electron-Laser Light.” *Phys. Rev. Lett.* **113**, 193201 (2014).
- [4.18] N. Rohringer, *et al.* “Stimulated X-Ray Raman Scattering with Free-Electron Laser Sources” *Springer Proceedings in Physics* **169**, 201 (2016), eds, Rocca, Jorge Menoni, Carmen Marconi, Mario.
- [4.19] Liu, J.-C., Sun, Y.-P., Wang, C.-K., Ågren, H. & Gel’ mukhanov, F. “Auger effect in the presence of strong x-ray pulses.” *Phys. Rev. A* **81**, 43412 (2010).

[4.20] Demekhin, P. V., Chiang, Y.-C. & Cederbaum, L. S. “Resonant Auger decay of the core-excited C\*O molecule in intense x-ray laser fields.” *Phys. Rev. A* **84**, 33417 (2011).

[4.21] Kanter, E. P. *et al.* “Unveiling and Driving Hidden Resonances with High-Fluence, High-Intensity X-Ray Pulses.” *Phys. Rev. Lett.* **107**, 233001 (2011).

# 5. Chemistry

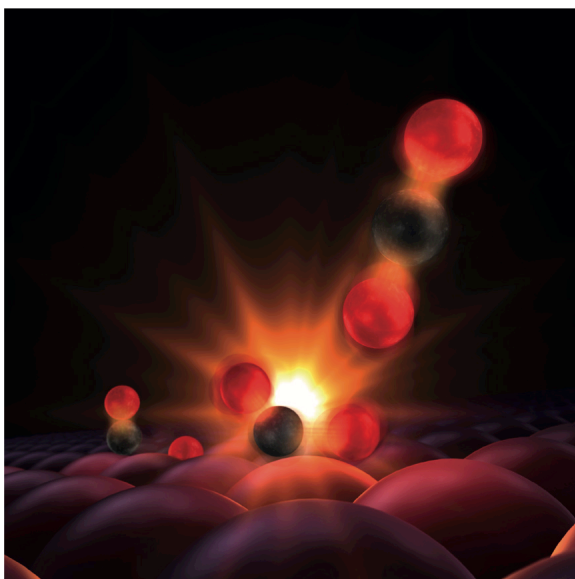


**Figure 5.1.** CO oxidation on Ru. (Reprinted by permission from SLAC National Accelerator Laboratory.)

The core of chemistry is reactivity and often we view this as kinetic phenomena where reactions are initiated in rare stochastic events. A fundamental understanding of chemical reactivity requires study of such reaction events through synchronization, which is possible by controlled initiation with light, and enables following the evolution of various excited electronic states, reaction intermediates and transition states. Together with the unique pump capabilities, SXL will enable us to probe how reacting molecules and excited states evolve on timescales of electronic and nuclear motion.

The ability to follow the dynamics is essential for elucidating important chemical processes strongly connected to challenges in society. Various forms of thermal- electro- and photochemistry are involved in every chemical energy transformation concerning energy storage, production and waste management. These processes hold some of the keys to a future sustainable society in applications such as solar cells, fuel cells or different catalysts. The

chemical industry is the largest in the world and it is responsible for about 10% of the industrial production measured in added value. Understanding processes on timescales relevant to observe bond breaking, bond formation and electron transfer is thus of utmost societal importance. Free electron laser studies will allow a transfer from static models of chemical processes to dynamic ones.

## 5.1 Photochemistry

- *How can electron dynamics be resolved in time and space?*
- *How can soft X-rays aid in the understanding of ultrafast excited state dynamics?*
- *How are electron and nuclear transfer dynamics coupled together?*

Photochemistry forms the knowledge fundament for understanding and controlling photoinduced chemical reactions and for the rational design of photovoltaic devices and photocatalysts. Photochemistry is also important in the atmosphere, where solar radiation creates radicals, such as OH, and atomic O and Cl, which play important roles in processes such as smog formation and ozone depletion. Time-resolved studies using SXL will provide information about reaction rates and intermediates, which is crucial for describing such processes in atmospheric models.

A developed framework for controlling the outcome of complex ground state chemical reactions exists, guiding for example organic synthesis. A fundamental challenge in photochemistry is to extend our understanding beyond the framework of potential energy surfaces, which serves nearly all ground state

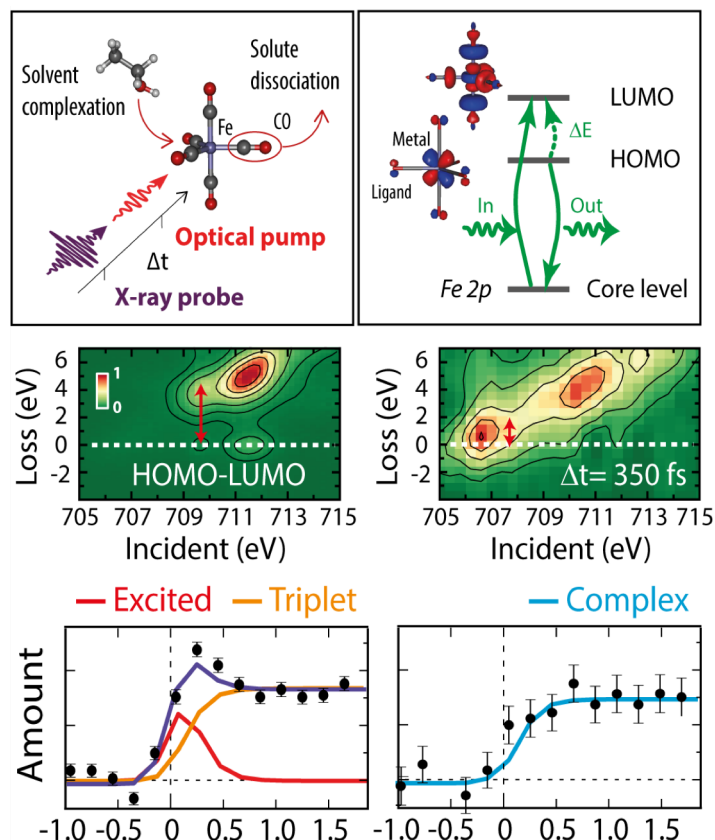


**Figure 5.2. Top:** Schematic showing the optical pump/X-ray probe experiment where excited-state evolution in CO dissociating from  $\text{Fe}(\text{CO})_5$  in solution was probed using RIXS at the free electron laser LCLS in the USA. An optical pump pulse was used to trigger CO dissociation from  $\text{Fe}(\text{CO})_5$  in solution and a subsequent femtosecond soft X-ray pulse to probe the excited-state evolution of the system. (left). Energy level diagram of the RIXS process. By measuring the energy loss of the scattered photons ( $\Delta E$ ) the frontier orbitals are probed directly.

**Middle:** Measured RIXS intensities (red corresponds to intensities normalized to one, green are intensities equal to zero) for  $\text{Fe}(\text{CO})_5$  (left) and photoproducts at a pump-probe delay of 350 fs.

**Bottom:** An electronically excited singlet state converts into a triplet state of  $\text{Fe}(\text{CO})_5$  on a sub picosecond timescale with concomitant formation of a singlet complex with the solvent (filled circles are measured data, lines represent a fitted kinetic model). (Figure 5.2 reprinted by permission from K. Kunnus and Ph. Wernet, HZB. Copyright (2016).)

chemistry, but often fails for excited states reactions. In particular, photochemistry involves non-adiabatic processes and intermolecular charge transfer processes occurring simultaneously as proton transfer and solvent dynamics. The aim is to extract simple principles for excited state dynamics and, in the longer run, for molecular design.

In fig. 5.2, it is shown how femtosecond time-resolved RIXS was used to reveal the excited-state dynamics of a benchmark transition-metal complex in solution [5.1]. In (Fe L-edge) RIXS, incident soft X-ray photons promote Fe 2p electrons to the lowest unoccupied molecular orbitals (LUMO). Electrons from the highest occupied molecular orbitals (HOMO) fill the core hole and may emit soft X-ray photons. By measuring the energy loss of the scattered

photons ( $\Delta E$ ) the frontier orbitals are probed directly. These insights are enabled by the ability of femtosecond X-ray spectroscopy to map, with atom specificity, frontier-orbital interactions that lie at the heart of chemical transformation. In this example, SXL would expand the accessible timescale down to the few-femtosecond regime. An SXL experiment would therefore allow us to probe the early evolution in the excited state landscape and to precisely monitor the structural change at an initial stage, giving insight into the coupling of electronic and nuclear degrees of freedom.

Photoinduced electron transfer is at the very heart of any photophysical and photochemical process in biological systems as well as in artificial light harvesting systems for photovoltaic and photocatalytic devices. In the example in fig. 5.3, time-resolved X-ray spectroscopy at the SPring-8 Angstrom Compact Free Electron Laser (SACLA) in Japan was used, in combination with

optical femtosecond spectroscopy, to unravel the time evolution of the excited state processes in a bimetallic chromophore [5.2]. It is a clear demonstration of how X-ray probes can be used to overcome the limitations of optical spectroscopy, which rely on the availability of optically allowed valence transitions. Moreover, X-ray probes are intrinsically local due to the involvement of core electrons and can thus be used to pinpoint dynamic processes not only in time, but also in space in a straightforward manner. A soft X-ray free electron laser such as SXL would offer the possibility of extending the observable timescale down to femtoseconds which would allow direct probing of the metal-to-ligand charge transfer excitation. SXL would also allow the spatial probing of these dynamics at essentially any site of the chromophore, since the energy range allows the (resonant) probing of the K-shell excitations of both low-Z elements (C, N) as well as L-shell/M-shell excitations of the 3d/4d transition elements (Co/Ru).

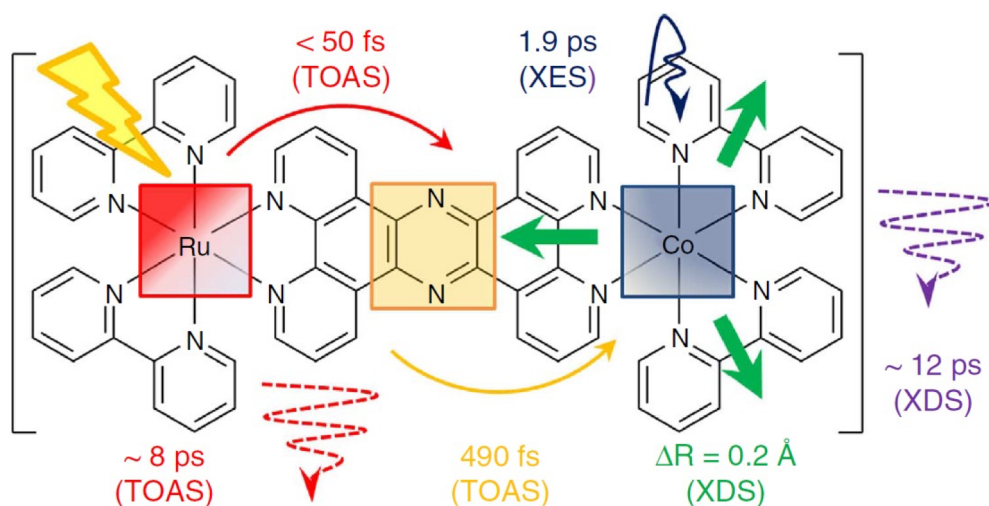


**Figure. 5.3.** Transient optical absorption spectroscopy (TOAS), time-resolved X-ray emission spectroscopy (XES), and time-resolved X-ray diffuse scattering (XDS) were investigated to study the electron transfer in a prototypical binuclear electron-harvesting chromophore. An upper limit of 50 fs was determined for the metal-to-ligand charge transfer (MLCT) excitation from the Ru moiety towards the bridging unit. (Reproduced from Ref. [5.2].)

## 5.2 Heterogeneous catalysis

- *How do ultrashort-lived intermediates and transition states determine activity and selectivity in heterogeneous catalysis?*
- *How do non-adiabatic electron dynamics affect catalytic reactions?*
- *Is it possible to go beyond the material limitations and develop new catalysts based on a fundamental understanding of dynamics?*

Nearly all of the industrial chemical processes involved in energy conversion use catalytic chemical transformations at interfaces between solids and liquids or gases. At the same time it is essential to develop a sustainable chemical industry that uses natural resources optimally. This can be achieved by developing novel catalytic materials with enhanced activity and selectivity, which in turn depends on a microscopic atomic-level understanding of the processes involved. A catalyst works by changing the electronic structure of the reacting species and thus lowering energetic barriers in the reaction, see the left panel of fig. 5.4. The transition state is at the highest energy point in the reaction path and separates reactants from products or the

various intermediates and controls the kinetics of the overall process. Catalysis needs to be studied in terms of dynamical competition between many reaction pathways that occur on ultrafast timescales at the interface. The number of molecules that react at a specific time during a catalytic reaction is usually very low and short-lived intermediates and transition states cannot be studied under steady-state conditions. In order to understand the reaction mechanisms the transient short-lived intermediates have to be detected and characterized on ultrafast timescales, which can be done using pump/probe techniques. Figure 5.4 shows such an example where ultrafast X-ray emission (XES) and absorption (XAS) spectroscopy at LCLS was used to observe CO oxidation on Ru. Here both a transient weakly interacting precursor state and the transition state in a catalytic surface reaction were detected on the electronic structure level [5.3, 5.4]. To achieve a full understanding of heterogeneous catalytic reactions, information on the dynamics of making and breaking bonds at interfaces in terms of the individual atomic and molecular forces and the motions that these forces induce during chemical change is also necessary. It is therefore important to also study charge and energy flow in the surface region during each individual elementary reaction step.

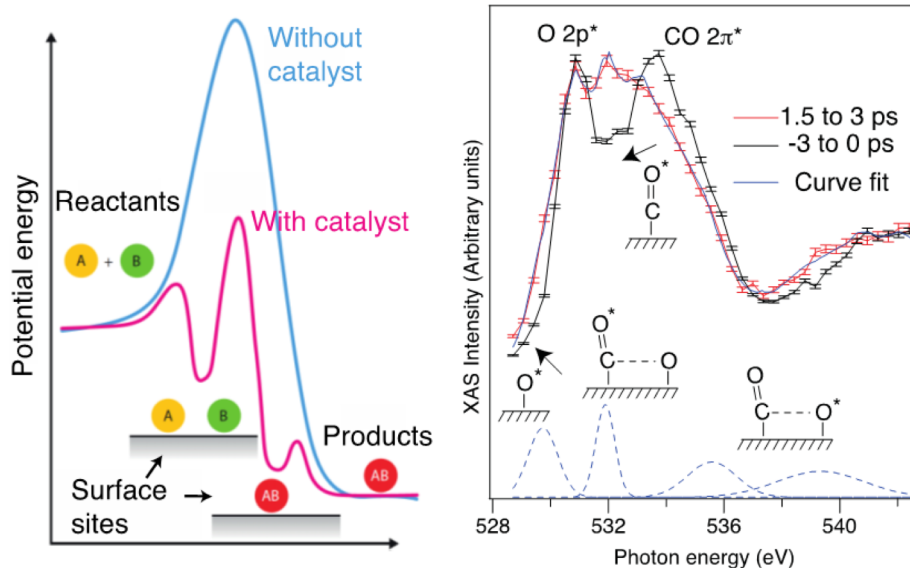


**Figure 5.4. Left:** Schematic picture of the potential energy surface of a gas phase reaction with a larger barrier and a more efficient surface catalytic reaction from reactants to products via 2 different intermediates and 3 smaller barriers. **Right:** X-ray absorption spectra of the adsorbed reactants CO and O before reaction is initiated by a femtosecond laser pulse (black) and 1.5 to 3 ps after the pump with a substantial population of molecules around the CO oxidation transition state. (Right figure reprinted by permission from AAAS. Östrom, H. et al., *Science* **347**, 978 (2015), copyright (2015).)

With SXL, novel pumping-schemes in combination with core-level spectroscopic probing can be envisioned to become important to determine these energy-flow mechanisms. On the one end of the spectrum short THz pulses can provide a tool to modify the electronic structure and induce non-adiabatic energy flows during reactions by strong electric fields [5.5]. On the other end of the spectrum soft X-ray pulses will provide a spatially localized pump that can selectively excite subsets of adsorbed molecules using core-level excitation. In between these extremes SXL can provide further insights into reaction mechanisms using far- and mid-infrared pump pulses that excite reactions via external adsorbate vibrations (phonons), near-infrared pulses that are often used to excite surface

reactions via hot substrate electrons or visible to ultraviolet pulses that can excite reactions via direct non-thermal electronic excitation.

### 5.3 Electrochemistry

- *What mechanisms govern the proton transfer in electro-catalysis?*
- *Is charge and proton transfer sequential or concerted (fig. 5.5)?*
- *What is the nature of the transition state in proton transfer assisted surface chemistry?*

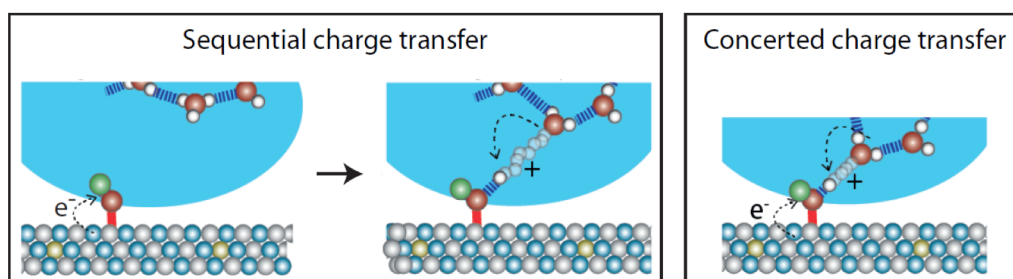


**Figure 5.5.** Schematic figure showing sequential (**left**) and concerted (**right**) oxidation-reduction reaction.

Heterogeneous chemistry at the liquid-solid interface is associated with challenging future catalytic processes based on electrochemistry, such as transforming  $\text{CO}_2$  to fuels and nitrogen to ammonia using electricity produced by renewable resources, as well as in today's fuel cell technology, which allows converting chemical energy of fuels, such as hydrogen, hydrocarbons and alcohols, into electricity. An energy efficient operation of these chemical fuel production and utilization reactions requires efficient and selective electron and proton transfer at the liquid-solid interface. In spite of intensive studies for over one hundred years and in spite of the importance of the charge transfer process at the liquid-solid interface in electrocatalysis, this process remains poorly understood at a microscopic level.

The structure and dynamics of the electrochemical interface are altered by the presence of an external voltage which attracts/repels ions near the electrode surface. The electric field in the layer influences the transition-state energy of the electrochemical reaction as reactant ions and molecules as well as the electrode surface undergo solvation and desolvation to reach the transition point. At the transition point, electrochemical reaction theory assumes adiabatic electron-transfer between the electrode and reactants. The rate of this electron transfer (the exchange current) determines the electrochemical catalytic activity.

Soft X-ray characterization of molecular configurations and oxidation states and establishing relevant timescales in electrochemical reactions will advance the present concepts and accelerate the development of new catalytic processes. Relevant processes span a wide range of timescales from the slow initial reorganization of nuclear and solvent coordinates, to the establishment of the transition point configurations, and the subsequent fast electron transfer between the electrode and the reactant molecules/ions. The latter steps are difficult to access with present X-ray sources.

Oxidation-reduction reactions may occur either sequentially or concertedly, see fig. 5.5. In the first case either the electron or proton transfers first which produces a charged intermediate state that attracts oppositely charged species in the electrolyte. After the association of the reactants, they react together in the second charge transfer step. In the concerted reaction, on the other hand, the electron and proton transfer simultaneously without a stable intermediate. Indeed, concerted mechanisms have been recognized as important in chemistry and biology and play a critical role *e.g.* in photosynthesis [5.6, 5.7]. Here, pre-association of the reactants is required before the electron-proton transfer due to the short-range nature of proton transfer. The pre-association of reactants with hydrogen-bonding may avoid a significant structural reorganization during the electron-proton transfer.

SXL will allow studying charge transfer mechanisms at electrochemical interfaces with the goal to identify the state of the molecules at the transition point and distinguish between the sequential and proton-coupled/oxygen anion-coupled electron transfer mechanisms. Electrochemical cells [5.8, 5.9] will be adapted for ultrafast time-resolved X-ray absorption and X-ray emission spectroscopy measurements.

To initiate the charge transfer on a sub-ps timescale, THz radiation at SXL will be used with ultrashort half-cycle pulses that give an electric field pulse that can induce a charge migration at the interface to provide momentum along a specific reaction coordinate on an ultrafast timescale [5.5]. Using the strong electric field of THz radiation, the electrochemical reaction will be steered through migration of either electrons in the solid or ions in the liquid.

## 5.4 Photovoltaics

- *What is the atomic scale mechanism for energy dissipation in photovoltaic materials?*
- *How can material properties be designed for non-equilibrium processes to be directed at the interface or at the nanoscale?*
- *What can be generalized or will the answers to the questions above always be specific for a chosen type of photovoltaic material?*

The conversion mechanism in different heterojunction and molecular (dye-sensitized) solar cells starts with light absorption and is followed by charge separation and subsequent charge injection to a conducting material. Recently new families of photovoltaics have been developed with promising efficiencies in the 12-25% range that are based on organic and inorganic materials with properties that can be fine-tuned. The conversion efficiency in the traditional dye-sensitized nanostructured solar cells depends on light absorption, on the success

in injecting charges to the different materials and on the possibility to limit the losses due to different recombination routes over the interface. Recent developments involve new hole-conducting materials transferring the liquid photoelectrochemical cells into solid state devices highly related to classical organic solar cells. Also, the introduction of so-called perovskite materials as both photon absorbing and charge-transporting materials has boosted conversion efficiencies, albeit a fundamental understanding is in many cases missing [5.10, 5.11]. The mechanism of conversion in organic excitonic solar cells (see fig. 5.6) depends on exciton diffusion and subsequent charge separation by dissociation. For thin films the conversion is modeled by photogeneration of electron hole-pairs and separation because of the internal electric field created by the diode structure at a heterojunction. In all cases the mechanisms include energy dissipation, diffusion and interfacial charge transfer reactions and the overall efficiency largely depends on the competition between different reactions in different time regimes where an appropriate energy level alignment at the interface is necessary to allow for charge separation. SXL can provide insight, required to predict functional properties and improve efficiencies, by following the response and evolution of the electronic structure in complex solar cell materials after photon irradiation. Time-resolved soft X-ray spectroscopies will be used to map the dynamical changes in the electronic structure of the materials on a picosecond and femtosecond timescale, not possible at synchrotron sources. The feasibility of femtosecond photoemission spectroscopy (PES) studies has been tested by X-ray free electron laser experiments. Time-resolved carbon 1s PES experiments on N3 dye-sensitized ZnO semiconductor nanocrystals have been performed at the LCLS FEL. This type of measurements, still at the early stages, revealed to be quite difficult because the optical pump causes modifications of the line shapes of the measured core levels due to space charge effects that can be quite severe and obscure the interesting dynamics.

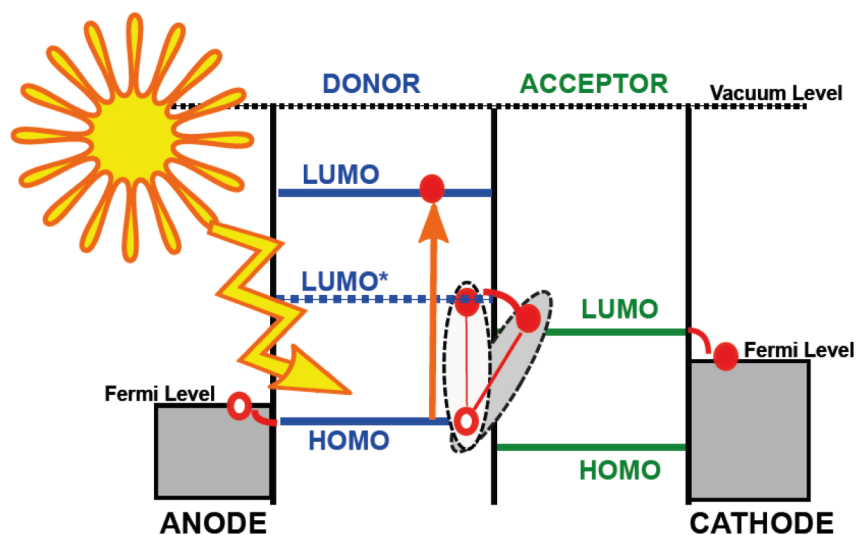


**Figure 5.6.** Working principle of an organic photovoltaic device, indicating interfaces of importance for charge separation. (Reprinted by permission from M. Dell'Angela, CNR-IOM.)

SXL will be well suited for studying femtosecond time-resolved RIXS to determine the picosecond and femtosecond dynamics of the electronic structure in D/A (donor/acceptor) systems. The optical pump (190-2600 nm) will mimic the sunlight, while the soft X-ray probe (RIXS) offers the advantages of chemical

selectivity of core level spectroscopies. The extension of RIXS into the time domain offers unprecedented experimental possibilities in the study of organic solar cells where the presently available information at equilibrium can now be extended.

## References

- [5.1] Wernet, P. *et al.* “Orbital-specific mapping of the ligand exchange dynamics of Fe(CO)<sub>5</sub> in solution.” *Nature* **520**, 78–81 (2015).
- [5.2] Canton, S. E. *et al.* “Visualizing the non-equilibrium dynamics of photoinduced intramolecular electron transfer with femtosecond X-ray pulses.” *Nat. Commun.* **6**, 6359 (2015).
- [5.3] Östrom, H. *et al.* “Probing the transition state region in catalytic CO oxidation on Ru.” *Science* **347**, 978–982 (2015).
- [5.4] Dell’angela, M. *et al.* “Real-Time Observation of Surface Bond Breaking with an X-ray Laser.” **339**, 1302–1305 (2013).
- [5.5] LaRue, J. L. *et al.* “THz-Pulse-Induced Selective Catalytic CO Oxidation on Ru.” *Phys. Rev. Lett.* **115**, 36103 (2015).
- [5.6] Huynh, M. H. V. & Meyer, T. J. “Proton-Coupled Electron Transfer.” *Chem. Rev.* **107**, 5004–5064 (2007).
- [5.7] Weinberg, D. R. *et al.* „Proton-Coupled Electron Transfer.” *Chem. Rev.* **112**, 4016–4093 (2012).
- [5.8] Sanchez Casalongue, H. G. *et al.* “In Situ Observation of Surface Species on Iridium Oxide Nanoparticles during the Oxygen Evolution Reaction.” *Angew. Chemie Int. Ed.* **53**, 7169–7172 (2014).
- [5.9] Casalongue, H. S. *et al.* “Direct observation of the oxygenated species during oxygen reduction on a platinum fuel cell cathode.” *Nat. Commun.* **4**, (2013).
- [5.10] Zhao, Y. *et al.* “Organic–inorganic hybrid lead halide perovskites for optoelectronic and electronic applications.” *Chem. Soc. Rev.* **45**, 655–689 (2016).
- [5.11] Collavini, S., Völker, S. F. & Delgado, J. L.” Understanding the Outstanding Power Conversion Efficiency of Perovskite-Based Solar Cells.” *Angew. Chemie Int. Ed.* **54**, 9757–9759 (2015).

## 6. Condensed Matter Physics

---

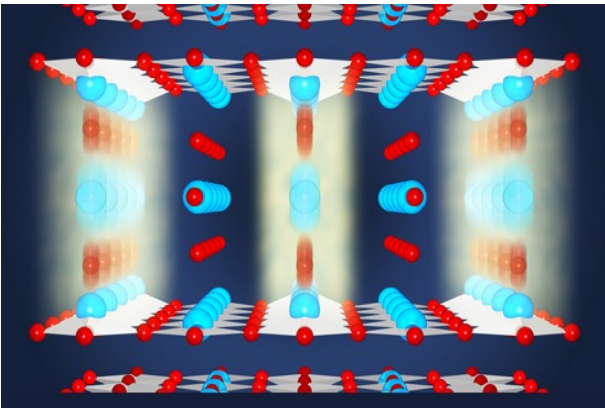


**Figure 6.1.** *Illustration of the laser induced vibration of oxygen atoms between layers of copper oxide in YBCO which causes structural changes that favor superconductivity. [6.1] (Reprinted by permission from Jörg Harms, Max Planck Institute for the Structure and Dynamics of Matter.)*

Condensed matter physics deals with understanding matter in its condensed form, typically divided into “hard” and “soft” phases. Conventional, or “hard”, condensed matter physics focuses on the properties of the solid states, while “soft” condensed matter deals with the properties of polymers, gels and liquids. The SXL beamline will be able to tackle challenges in both research fields, by providing coherent and intense light at the photon energies of the C, N and O K-edges, and of the Mn, Fe, Co, Ni and Cu L-edges.

Modern “hard” condensed matter physics research aims at designing and controlling materials (fig. 6.1) that will eventually push technology beyond the limits of silicon. In fact, today’s information society is increasingly

dependent on the availability of faster communication in ever-smaller devices. In the past half century, this demand has been satisfied by silicon-based semiconductor technology, which has been able to follow the pace dictated by Moore’s law [6.2]. However, it is now evident that such a trend is coming to an end [6.3, 6.4], and that new fundamental ideas will be needed to sustain technological progress. In addition, those new ideas will need to address the issue of energy efficiency, at the basis of a sustainable life on Earth. In practice, the quest is towards finding ways to manipulate and detect suitable material properties using the least amount of energy, at the fastest times and at the nanoscale. Succeeding in this task would enable devices that are not only more compact, but also more powerful and less energy-hungry. Ultimately, this will lead to devices and technologies that will sustain human progress.

Soft matter physics is usually related to disordered systems such as polymers, colloidal systems, gels, glasses and liquids. These undergo rearrangements on many different length and timescales that are intricately related to the fundamental function and, as illustrated in fig. 6.2, will strongly benefit from coherent X-rays. Here we will mostly focus on glasses and liquids that provide some of the core questions in condensed matter physics regarding the nature of the glass transition and if there can exist several macroscopic phases in supercooled liquids that are inherently metastable. SXL can be unique in probing the collective fluctuations of such systems based on coherent scattering and spectroscopy.

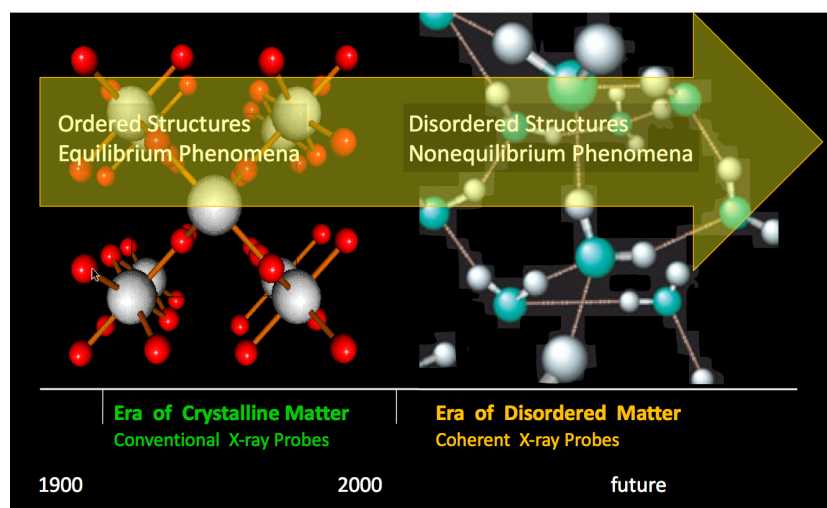


**Figure 6.2.** Illustration of the possibilities for studies of disordered structures enabled by the development of coherent X-ray probes. (Reprinted by permission from Helmut Dosch, DESY.)

## 6.1 Ultrafast magnetism: watching spins move in time and space

- How is angular momentum conserved on ultrafast timescales?
- Can we directly detect ultrafast spin currents and measure their mean free path?
- Is nanoscale (dis)order a key ingredient for the occurrence of ultrafast demagnetization?

In the field of ultrafast magnetism, one primary aim is to develop methods to manipulate the building blocks of magnetism (spins) on the nanoscale with a focus on speed and energy efficiency. Energy efficiency arises from the fact that, at ultrafast timescales, one can aim at “beating” other, slower dissipation channels. The other two characteristics, the nano-scalability of a spin device and its speed, are plausible thanks to the fact that magnetism is controlled by exchange and spin-orbit interactions, which act at the femtosecond timescales and within atomic distances. Figure 6.3 illustrates the challenges of detecting the spin transport that lead to ultrafast magnetization changes over nanometer distances [6.5].

The research field started in 1996 with the pioneering experiments of Beaurepaire *et al.* [6.6], who discovered experimentally that femtosecond laser pulses can **quench** the magnetization of a thin-film ferromagnet on timescales below 1 ps. Ten years later, Stanciu *et al.* demonstrated all-optical **switching** of

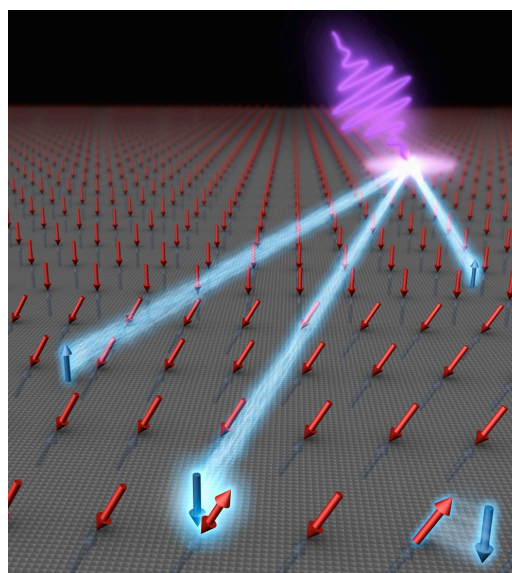


**Figure 6.3.** Illustration of how laser light incident on the sample generates iron spin currents that transfer their angular momentum to gadolinium spins on a nanoscale region. (Reprinted by permission from SLAC National Accelerator Laboratory.)

magnetization in a ferrimagnet [6.7]. Very recently magnetization reversal in a ferromagnet has also been demonstrated [6.8], opening up for the opportunity of ultrafast magnetic data storage controlled by light. Furthermore, theoretical efforts in Sweden have led to the prediction [6.9, 6.10] of ultrafast spin currents transcending the demagnetization event. This opens up the exciting prospect of the non-local manipulation of magnetization [6.5]. However, despite the fact that these phenomena have now been explored extensively both theoretically and experimentally, ***the physics of ultrafast demagnetization is still puzzling and there is no consensus over what is the mechanism through which a magnetic system can dissipate angular momentum at such fast timescales.*** The complexity of this problem lies in the non-equilibrium character of the physics at play, and in the strong coupling of the many degrees of freedom that are all simultaneously excited during ultrafast demagnetization.

The unique characteristics of the SXL beamline at MAX IV will open up for

experiments that may help unveiling these fundamental questions. The availability of circularly polarized X-ray photons will allow for quantitative measurements of the spin and orbital angular momentum via the sum rules applied to the X-ray magnetic circular dichroism (XMCD) signal [6.11, 6.12] at the resonant L-edges of  $3d$  metals. The possibility of realizing pump-probe experiments with a widely tunable pump (in particular with the availability of THz photons) will enable time-resolved experiments with femtosecond resolution where the coupling between spin currents and demagnetization can be identified [6.13]. Finally, the coherent nature of the X-ray photons produced at SXL will allow for coherent scattering and imaging experiments that combine femtosecond timescales and nanometer resolution [6.5, 6.14] (see fig. 6.4). Such endeavors are also expected to greatly benefit from the progress in the technique of resolution enhancement via phase retrieval. Following demonstration with visible light [6.15], such technique has been applied to coherent X-ray diffraction [6.16, 6.17].

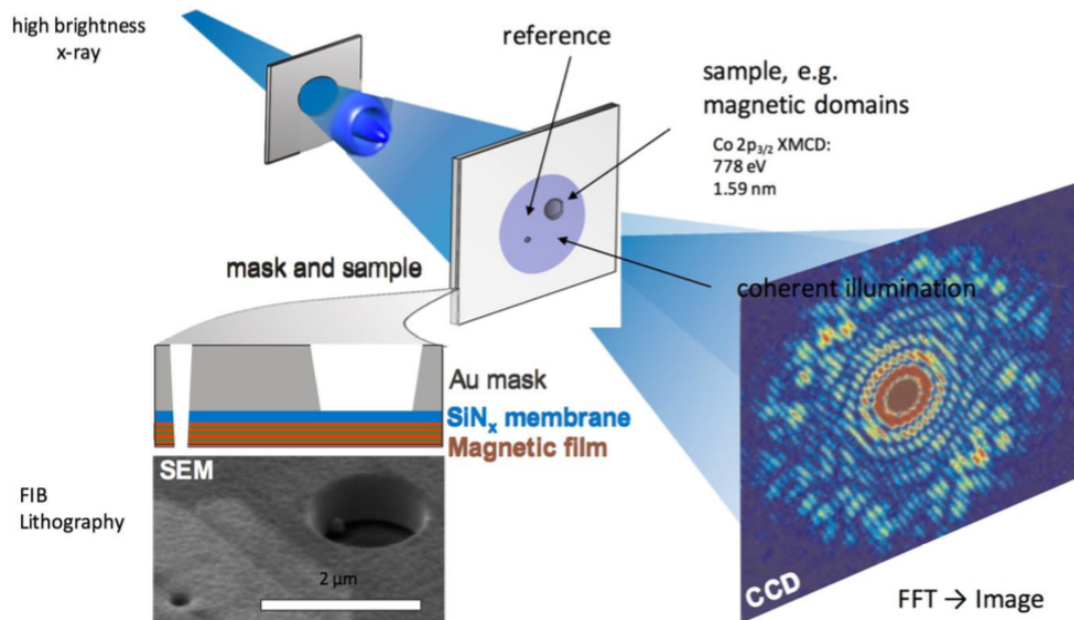


**Figure 6.4.** Schematic of a holographic imaging experiment that would be possible thanks to the coherent nature of the SXL radiation. SXL will also allow for time-resolved imaging using pump-probe schemes that can be combined with holographic measurements. [6.18] (Reprinted by permission from Macmillan Publishers Ltd: Nature. Eisebitt, S. et al., Nature 432, 885 (2004), copyright (2004).)

Finally, the possibility to produce coherent X-ray pulses of different colors and using them for pump-probe experiments has opened new excitation routes. One can perform so-called double resonance dynamic studies tuning the pump X-ray pulse to a selected electronic excitation of element A and probing with the second X-ray pulse tuned to an electronic resonance of element B. Such multi-color pump-probe schemes allow for studies of possible direct or indirect A-B coupling mechanisms following the evolution of transient states in low density and condensed matter and in many other research fields. Multi-color X-ray options are very promising for exploring dynamic processes in transition metal (TM) oxides [6.19] and other complex magnetic materials, as TM-rare earth compounds [6.20], where the presence of localized orbitals and the mediated coupling are expected to result in different magnetization dynamics induced by a resonant and non-resonant pump pulse. This was demonstrated recently comparing the behavior of magnetic samples with delocalized orbitals, permalloy (NiFe), and highly localized orbitals, NiFe<sub>2</sub>O<sub>4</sub> [6.21]. The O-mediated coupling in NiFe<sub>2</sub>O<sub>4</sub> could be sensibly affected by tuning the pump energy to a specific electronic excitation, Fe 3p resonance in this case.

## 6.2 Correlated systems - Superconductors

- *What is the mechanism behind high-temperature superconductivity and other emergent phenomena in correlated systems?*
- *What is the role of nanoscale phase separation?*
- *Can we use intense light fields to guide materials into structural phases not normally thermodynamically accessible?*

Correlated systems constitute a class of materials which display a wealth of physical phenomena that are both of strong fundamental interest and important for potential technological applications. A few examples are given by magnetism, metal-to-insulator transitions, superconductivity and heavy fermions. Additionally, the recent discovery and strong interest in topological matter have opened paths to new correlated topological systems, such as topological Kondo insulators and topological superconductivity [6.22].

One prominent example of an open research question within the field of correlated systems is the high-temperature superconductivity in copper oxides. The cuprates display rich phase diagrams and are characterized by the existence of competing phases such as charge ordering, the antiferromagnetic Mott insulator phase, the pseudogap phase and superconductivity. The complexity of these systems also reflects itself in their spatial properties, where both chemical and electronic inhomogeneities exist on a nanoscale [6.23]. For instance, spatial maps of the superconducting gap in the Bi<sub>2</sub>Sr<sub>2</sub>CaCu<sub>2</sub>O<sub>8+d</sub> system reveal a strong variation in the size of the gap across its surface [6.24-6.26]. These variations occur on a nanometer length scale and indicate that the coupling between real and momentum space might be an important property that holds the key to understanding these and other correlated systems. In other words, ***one of the key challenges in this field is to investigate how nanoscale phase separation and local chemical or electronic variations influence the functional properties of the materials.***

Understanding such interplay between competing phases requires, in turn, an understanding of the spatial properties and relevant length scales of the system. To describe the dynamic response of the system, one also has to identify the intrinsic timescales of competing dynamic processes.

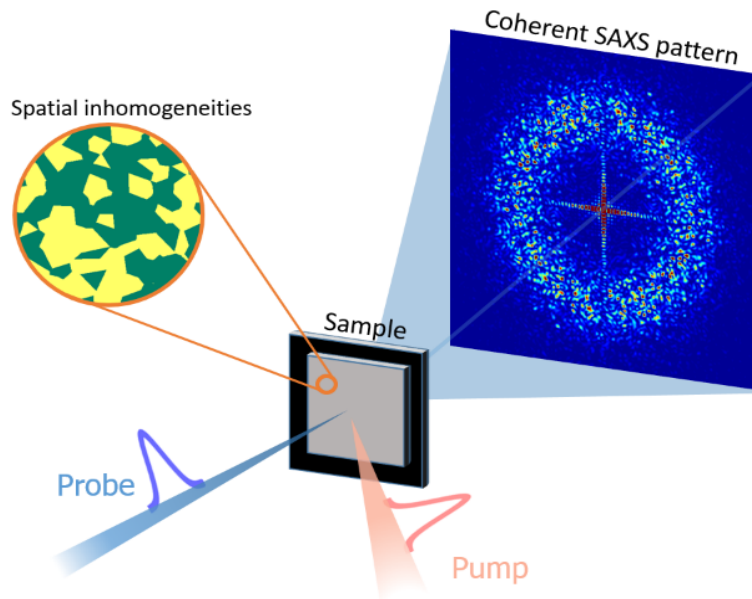


**Figure 6.5.** Schematic overview of a resonant coherent small-angle X-ray scattering (SAXS) experiment where dynamics in a spatially inhomogeneous sample are measured using a pump-probe setup. (Reprinted by permission from M. H. Berntsen, KTH.)

All of *this mandates experimental techniques that combine high spatial and temporal resolutions, with additional chemical specificity*. Such requirements are only met by the recently developed X-ray free electron lasers, and in particular the proposed SXL beamline. The fully coherent radiation and femtosecond time resolution of the SXL beamline, in conjunction with a wide variety of pump sources, will permit time-resolved resonant coherent scattering studies from many correlated systems with nanoscale phase separation. Ultrafast dynamics can then be captured by optical pump – X-ray probe experiments, but the coherent properties of the beam also open up for studying dynamics of spatial or electronic origin by the use of higher-order correlation functions [6.27].

In particular, by pumping cuprates with THz radiation tuned to specific low-lying excitations, such as phonons, we envisage driving a system between the normal and superconducting state – as demonstrated by D. Fausti *et al.* [6.28]. The spatial response of the system on the nanoscale can then be followed through the transition by resonant coherent scattering performed at the

oxygen K-edge, see fig. 6.5. Such experiments have not been performed to date and could provide completely new insights.

### 6.3 Correlated systems - Multiferroics

- *How can we use nonequilibrium pathways to manipulate ferroic orders in materials?*
- *Can we use nonequilibrium responses to better understand how coupling drives emergent behavior in quantum materials?*
- *Can we achieve ultrafast switching of the magnetic ordering via electric fields?*

Multiferroics are materials where two or more long-range ferroic orders coexist. An important example is magneto-electric type II multiferroics, where (anti)ferromagnetism and ferroelectricity is strongly coupled. This class of materials is very interesting from a fundamental perspective, because several different microscopic mechanisms can give rise to such

coupling [6.29, 6.30]. These materials are also appealing from an applied perspective: magneto-electric multiferroics are ideal candidates where pure electric-field switching (*i.e.* with no current flow) of the magnetization can be realized. So called MeRAM have been proposed as a new type of memory that combines the advantages of magnetic and ferroelectric memory [6.31]. Despite these great perspectives, we still need to address fundamental questions: ***How can we switch multiferroic materials in an efficient way? How fast can we do this?*** A recent approach in trying to answer those questions is to use light as a control knob. Since the last decade, technology exists to finely tune laser pulses at IR and optical wavelengths. Even more recently, major steps forwards have been taken towards the production of bright laser sources at THz frequencies, which enables the resonant excitation of IR active modes. In turn, these two regions of electromagnetic radiation allow for two different strategies towards manipulating multiferroic order: indirect and direct.

***Indirect control.*** Using higher-energy photons, one can in some systems exert a measure of control over degrees of freedom which eventually couple to the ferroic order. An example of this approach is the control of the phase transition in cupric oxide (CuO) via an IR pulse which excites electronic states. CuO has a low-temperature antiferromagnetic, non-ferroic phase, and a high-temperature incommensurate spiral magnetic order that is coupled to the ferroelectricity [6.32]. Starting from the low-temperature phase, one can pump the system with a femtosecond IR pulse and observe the emerging multiferroic phase by looking at the resonant X-ray diffraction signal at the Cu L-edge. The pioneering experiment of [6.33] showed that indeed optical excitations can be used to drive the system into the multiferroic order, and that there exists an onset time of  $\sim 400$  fs before the transition can take place. Further experimental investigations into this and related systems are needed to understand better the details of the formation of this newly ordered phase, and SXL

will have the necessary characteristics to tackle these challenges.

***Direct control.*** While this method of indirect control works in some systems, there are important disadvantages in following this route: competing excitations often produce undesirable side effects (*e.g.* unwanted heating or material damage) that quite generally drive the system to a state with much higher entropy. A possibly better alternative is to exploit the presence of low-energy excitations to drive the ferroic order directly with an electromagnetic pulse, typically in the THz range [6.34]. Inspired by the theoretical predictions in [6.35], the feasibility of such an approach has been very recently demonstrated in terbium manganese (TbMnO<sub>3</sub>) [6.36] (fig. 6.6). In this study, the authors pumped a so-called electromagnon (*i.e.* a spin excitation that is electric-dipole active) with a THz pulse, and observed the response of the magnetic order by measuring the resonant X-ray diffraction signal at the Mn L-edge.

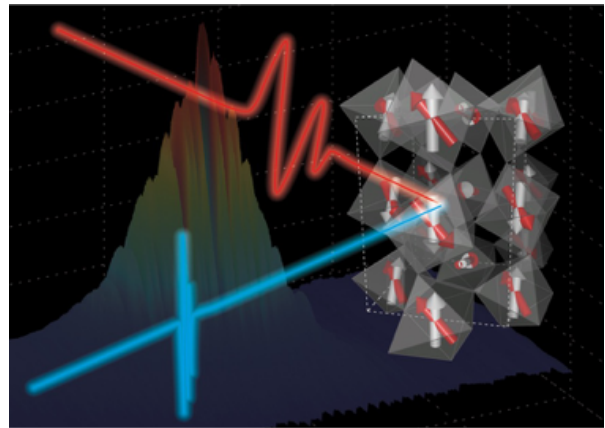


**Figure 6.6.** Schematic of a THz pump, soft X-ray probe experiment aimed at resonantly controlling and detecting the magnetic order in a multiferroic. (Reprinted by permission from T. Kubacka, ETH Zürich.)

Thanks to its characteristics, such as the availability of THz photons as a pump, the availability of circularly polarized photons, and the unique detection capabilities that may even

allow for imaging of magnetoelectric domains, the SXL will allow for such studies to directly address the problems of scaling these processes up to the level of general control over multiferroic polarizations. Magnetoelectric domain walls display intriguing physical properties, as for instance room-temperature electronic conductivity at ferroelectric domain walls in the insulating multiferroic  $\text{BiFeO}_3$ . In the type II multiferroic  $\text{Mn}_{0.95}\text{Co}_{0.05}\text{WO}_4$ , spin-driven ferroelectricity promotes the emergence of charged domain walls, which can be controlled by external magnetic fields. The observed behavior was explained by multiscale modeling combining first-principles density functional theory calculations and Landau-Lifshitz-Gilbert simulations [6.37].

## 6.4 Structure and dynamics of liquids and glasses

- *Can we address fast dynamics after THz pump using soft X-ray spectroscopy as probe in liquids?*
- *Are there unique dynamic heterogeneities in liquids and glasses?*
- *Can X-ray spectroscopy be used below the current limit of the core hole lifetime vibrational broadening?*

The physics of systems without translational invariance, such as liquids, dense fluids and glasses is one of the still intriguing questions in fundamental condensed matter physics that also connects with chemistry and biology. The understanding of the liquid-to-glass transition mechanisms, thermal anomalies at low temperatures, divergence of transport properties and relaxation phenomena is a challenge that motivates strong experimental and theoretical efforts. More recently also the concept of several macroscopic phases of liquids which have different densities and could give rise to a liquid-liquid critical point has become an important topic. In contrast to the crystalline case, in

disordered systems the understanding of inter- and intra-molecular dynamics is complicated not only by the difficulties associated with the absence of translational invariance, but also by the presence of other degrees of freedom such as, *e.g.*, diffusion and relaxation processes in fluids, or hopping and tunnelling processes in glasses. These processes naturally introduce different timescales, which are usually strongly dependent on the specific thermodynamic state. These timescales affect the collective dynamical properties differently, depending on their value as compared to the timescale characterising the particles vibrations around their quasi-equilibrium positions.

Water is of particular interest here since it is the key compound for our existence on this planet and it is involved in nearly all chemical, biological and geological processes. Access to clean water is one of the most challenging questions for mankind in the coming century, in particular with the prospect of climate change. Furthermore, water is involved in several energy related chemical transformations and is the key in many environmental processes. Although water is the most common molecular substance it is at the same time the most unusual one with many peculiar properties such as increased density upon melting, decreased viscosity under pressure, a density maximum at 4 °C, high surface tension and many more. In the low-temperature regime, below the freezing point, these properties deviate particularly strongly from those of a normal liquid. Several properties seem to diverge towards infinity at some mysterious temperature around -45 °C [6.38]. This has given rise to many proposals explaining the anomalous properties of water involving fluctuations of low density liquid (LDL) and high density liquid (HDL) local configurations that might lead to macroscopic phases in deeply supercooled water with a liquid-liquid transition (LLT) that ends in a liquid-liquid critical point (LLCP) [6.39-6.41], see fig. 6.7. Furthermore, water may also have several glass transitions from the amorphous phases [6.42]. One of the most essential questions to address for a

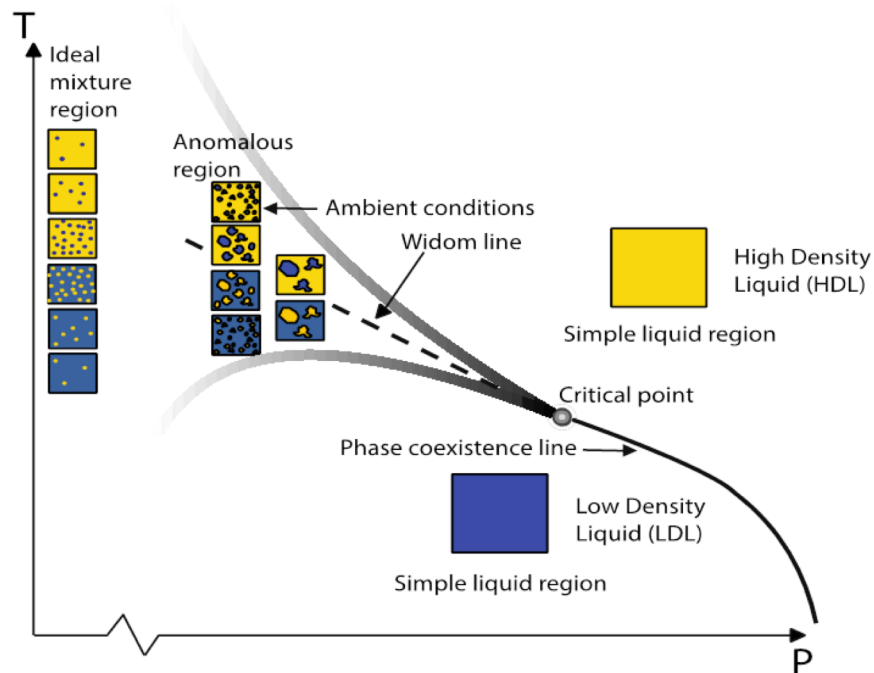


**Figure 6.7.** Schematic picture of a hypothetical phase diagram of liquid water showing the liquid-liquid coexistence line between LDL and HDL in terms of simple liquid regions, the critical point (real or virtual), the Widom line in the one-phase region and fluctuations on different length scales emanating from the critical point giving rise to local spatially separated regions in the anomalous region. The shaded lines indicate how far in temperature the fluctuations extend at the various pressures defining the anomalous region. (Reproduced from Ref. [6.39].)

microscopic understanding of water is: **What is the structure and dynamics of the hydrogen bonding (H-bonding) network in water that gives rise to all these unique properties?** This question has been discussed intensively for over 100 years but has not yet been resolved.

One scheme that can be utilised to probe liquid dynamics at the SXL is a THz pump – soft X-ray absorption spectroscopy (XAS) probe. The XAS spectrum of liquid water exhibits different spectral features that fingerprint distorted and strong H-bond configurations [6.43]. Therefore, by utilizing ultrafast soft X-ray pulses at different photon energies, one can selectively probe the dynamics of these different structural environments. Another way to probe water after THz excitation is using stimulated X-ray scattering schemes that offer interesting and promising possibilities due to their ability to

boost the efficiency of the naturally very photon-hungry techniques of conventional (spontaneous) resonant inelastic X-ray scattering and X-ray emission spectroscopy. More than that, using pulses that are significantly shorter than the natural Auger dominated core-hole lifetime, the decay of core-excited states can be stimulated at any time within the core-hole lifetime. This will open a sensitive tool to complement XAS in following THz induced dynamics in X-ray emission spectra [6.44].

By using soft X-ray coherent scattering one can access the low momentum transfer region with higher resolution and additionally implement spectral selectivity by changing the photon energy to probe resonantly the different peaks at the XAS spectrum. By combining this type of probe with a THz pump one can gain time-resolved information. Additionally, by

utilizing the large longitudinal and transverse coherence of the X-ray pulses one can get single-shot information of the instantaneous arrangement of the spatial heterogeneities by resolving the speckles of the recorded scattering pattern.

## 6.5 Semiconductor nanostructure dynamics: Dopants and interfaces

- *What are the properties of charge excitation, transfer and relaxation processes probed near impurities and interfaces?*
- *What is the correlation between impurity chemistry, vicinity to nanostructures and spin relaxation, electron-hole recombination, and local transport properties?*
- *Can nonlinear combinations of intense ultrashort light and X-ray beams be used to induce new functionalities in semiconductors?*

SXL will provide new insights into fundamental concepts such as electron screening, scattering, tunneling, coherence and excitation in low-dimensional compound semiconductor (nano) structures. Understanding electron dynamics in complex quantum confined low-dimensional structures is an important outstanding challenge in itself, but it will also have very real implications as one can study structures of proven relevance for future devices in IT, life science and renewable energy.

Looking at the properties of the SXL one realizes that there are a number of unique features that can be used for local studies of excitations and dynamics in semiconductors. Having access

to higher photon energies than available from conventional laser sources, it will be possible to use XAS to probe the dynamics of the local chemistry of specially implanted dopants (noticeably also magnetic dopants) and specially grown heterostructured interfaces during excitation. Even when no bond dissociation occurs, the excitation of the semiconductor with for example IR beams might influence the impurities (dopants) or vice versa. This can be directly combined with X-ray excited optical luminescence (XEOL) that can monitor the optical light emission with the added advantage of being chemical and excitation-channel specific [6.45, 6.46]. This is achieved by tuning the photon energy to a particular absorption edge of an element, thereby exciting preferentially those sites that will then be responsible for optical emission. Here a further salient feature of the semiconductors comes into play, since we can control the position of elements that determine optical or electrical function of the semiconductor. Semiconductor Silicon and III-V electronics and photonics are the central building blocks in virtually all electronic and optoelectronic devices used today. As a result, high developed platforms for synthesis and lithography of highly complex atomically controlled heterostructures exist. The state-of-the-art semiconductor heterostructure technology – allowing extremely precise tailoring of many different 2-dimensional (2D), 1D and 0D III-V semiconductor structures and total control of their surfaces, will be the sample foundation for studies. Thus, we can study a wide range of precisely controlled fundamental structural features (see fig. 6.8) such as geometric shape, crystal structure, composition and single-atom impurities and directly compare how they influence electronic structure and dynamics – also when added together in complex heterostructured patterns. We can now target specific parts of these structures with the element specificity of the SXL radiation.

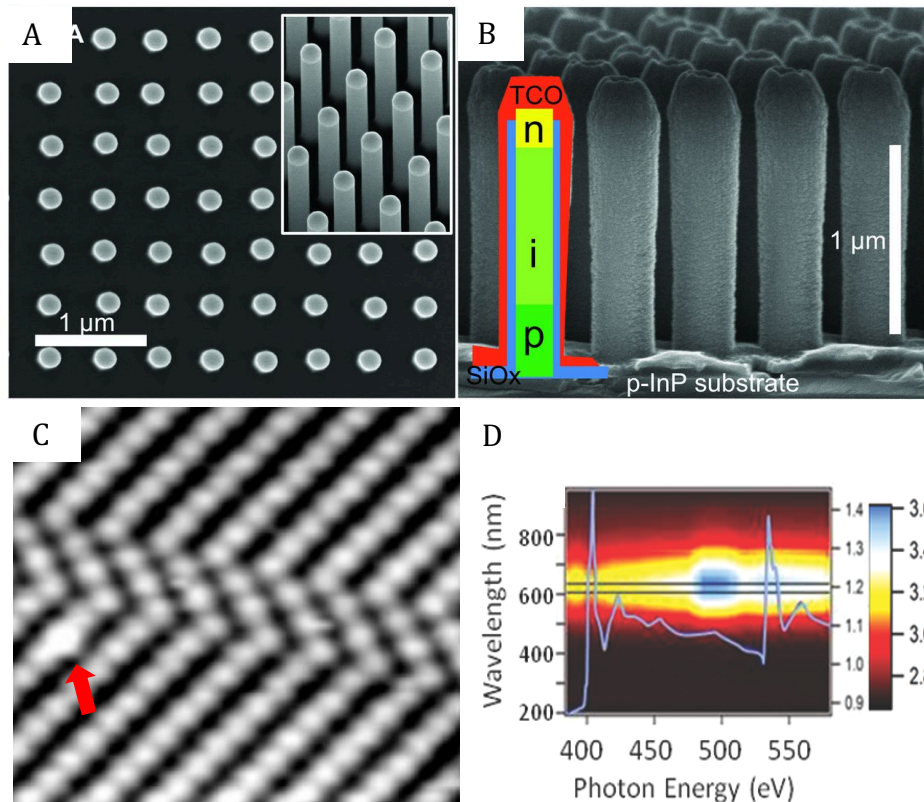


**Figure 6.8.** Example of semiconductor nanostructures from arrays to individual dopants. Many light elements are used for doping, Oxide/semiconductor interfaces are highly relevant and also magnetic elements such as Mn are used as dopants or interface layers. **(A) & (B)** Record efficiency InP Nanowire array solar cells: **(A)** 0° and 30° (inset) tilt SEM (scanning electron microscopy) images of as-grown nanowires with a surface coverage of 12%. **(B)** Interior doping structure of the nanowires, dopants were S and Zn. The wire is surrounded by various oxides for insulation and contacts. [6.47] (Figure A and B reprinted by permission from AAAS. Wallentin, J. et al. *Science* **339**, 1057 (2013), copyright (2013).) **(C)** STM (scanning tunneling microscopy) image of the Arsenic lattice inside a GaAs nanowire. The red arrow indicates a single C dopant inside the nanowire in close vicinity to a crystal twinning defect. [6.48] (Reprinted by permission from Macmillan Publishers Ltd: *Nature*. Mikkelsen, A. et al. *Nat. Mater.* **3**, 519 (2004), copyright (2004).) **(D)** 2D XANES-XEOL (X-ray absorption near-edge structure-XEOL) map of GaN:ZnO nanostructures. Mapping is across the N and O K-edges with total electron yield overlaid (blue). [6.49] (Reprinted by permission from John Wiley & Sons, Inc., Sham, T.-K. *Advanced Materials* **26**, 7896 (2014), copyright (2014).)

Combining SXL with THz excitation is also highly interesting for semiconductors. THz spectroscopy has long been used for carrier dynamics in semiconductors [6.50] and the addition of the SXL pulses opens up new opportunities. Again the opportunity to target specific dopants for compositional interfaces appears to be a key novelty. A final means of detection will be the insertion of semiconductor

devices directly in the beam and the monitoring of the change in I(V) characteristics with and without the X-ray beam. This can be combined with the THz signal which can be used to open and close a tunnel device [6.51].

The extremely short pulses conceivably available from the SXL would also be interesting in combination with ultrafast high repetition rate

laser sources. These have lower energy (1-90 eV), but can potentially reach pulse lengths from a few femtoseconds to tens of attoseconds. This can then be combined with electron microscopy methods for spatial resolution [6.52-6.54]. The SXL would represent a very different source with its lower repetition rate, but much higher intensities and photon energies. As Sweden also has strong groups in the area of ultrafast lasers that are currently moving towards studies of semiconductors and other solid state structures a fertile ground exists for a significant user segment that would explore these complementary sources.

Finally, from a fundamental science perspective, it could be interesting to investigate how the excitation of semiconductors with extremely intense and ultrashort X-ray and optical light pulses affects the semiconductor properties, and how the tuning to specific absorption edges might alter the semiconductor materials during the application of the X-ray pulse. This could be used for optical control in the quantum regime with X-rays and optical light exploring nonlinear effects.

## 6.6 Sub-femtosecond opportunities in condensed matter

- *Can we detect Bloch oscillations?*
- *Can we use SXL to access the timescales of quantum transport?*

The availability of pulses in the  $\sim 1$  fs, or even attosecond, range at the SXL beamline will allow for exploratory experiments which are of great fundamental scientific interest, and that are out of reach at existing facilities. Within condensed matter, this would call for an attempt to study quantum transport phenomena in metallic systems, such as the occurrence of Bloch oscillations.

Bloch oscillations are one of the very first predictions from the quantum theory of solids, but they have yet to be observed in naturally occurring crystals. The theory states that, in a perfectly periodical crystal lattice, electrons that are accelerated by a uniform electric field will undergo an oscillatory motion. This oscillatory motion reflects the periodic nature of the crystal and, in turn, of the band structure: as electrons acquire larger and larger momentum, they reach the zone-boundary, their group velocity goes to zero, and then reverses moving towards the zone-center again. When this happens, electrons are effectively moving in the direction *opposite* to the applied electric field, violating Ohm's law.

To date, experimental realizations of Bloch oscillations have been limited to specifically engineered semiconducting heterostructures, *i.e.* artificial crystals. In naturally occurring crystals, such as transition metals, the electron scattering times in the  $\sim 10$  fs range have hampered experimental observations, because electrons dephase before any coherent motion can be detected. At the SXL beamline, we will have the capabilities of succeeding in this task and, more generally, to access the proper timescales for quantum transport.

## References

- [6.1] Mankowsky, R. *et al.* “Nonlinear lattice dynamics as a basis for enhanced superconductivity in  $\text{YBa}_2\text{Cu}_3\text{O}_{6.5}$ .” *Nature* **516**, 71–73 (2014).
- [6.2] Moore, G. E. “Cramming More Components onto Integrated Circuits.” *Electronics* 114–117 (1965).
- [6.3] Mack, C. “The multiple lives of Moore’s law.” *IEEE Spectrum* **52**, 31–37 (2015)
- [6.4] Waldrop, M. M. “The chips are down for Moore’s law.” *Nature* **530**, 144–147 (2016).
- [6.5] Graves, C. E. *et al.* “Nanoscale spin reversal by non-local angular momentum transfer following ultrafast laser excitation in ferrimagnetic  $\text{GdFeCo}$ .” *Nat. Mater.* **12**, 293–298 (2013).
- [6.6] Beaurepaire, E., Merle, J.-C., Daunois, A. & Bigot, J.-Y. “Ultrafast Spin Dynamics in Ferromagnetic Nickel.” *Phys. Rev. Lett.* **76**, 4250–4253 (1996).
- [6.7] Stanciu, C. D. *et al.* “All-Optical Magnetic Recording with Circularly Polarized Light.” *Phys. Rev. Lett.* **99**, 47601 (2007).
- [6.8] Lambert, C.-H. *et al.* “All-optical control of ferromagnetic thin films and nanostructures.” *Science* **345**, (2014).
- [6.9] Battiato, M., Carva, K. & Oppeneer, P. M. “Super-Diffusive Spin-Transport as a Mechanism of Ultrafast Demagnetization.” *Phys. Rev. Lett.* **105**, 027203 (2011).
- [6.10] Malinowski, G. *et al.* “Control of speed and efficiency of ultrafast demagnetization by direct transfer of spin angular momentum.” *Nat. Phys.* **4**, 855–858 (2008).
- [6.11] Stöhr, J. & Siegmann, H. C. *Magnetism*. **152**, (Springer Berlin Heidelberg, 2006).
- [6.12] Higley, D. J. *et al.* “Femtosecond X-ray magnetic circular dichroism absorption spectroscopy at an X-ray free electron laser.” *Rev. Sci. Instrum.* **87**, 33110 (2016).
- [6.13] Bonetti, S. *et al.* “THz-Driven Ultrafast Spin-Lattice Scattering in Amorphous Metallic Ferromagnets.” *Phys. Rev. Lett.* **117**, 87205 (2016).
- [6.14] Wang, T. *et al.* “Femtosecond Single-Shot Imaging of Nanoscale Ferromagnetic Order in Co / Pd Multilayers Using Resonant X-Ray Holography.” *Phys. Rev. Lett.* **108**, 267403 (2012).
- [6.15] Gao, P., Pedrini, G. & Osten, W. “Phase retrieval with resolution enhancement by using structured illumination.” *Opt. Lett.* **38**, 5204 (2013).
- [6.16] Kim, C. *et al.* “Resolution enhancement in coherent x-ray diffraction imaging by overcoming instrumental noise.” *Opt. Express* **22**, 29161 (2014).
- [6.17] Latychevskaia, T., Chushkin, Y., Zontone, F. & Fink, H.-W. “Imaging outside the box: Resolution enhancement in X-ray coherent diffraction imaging by extrapolation of diffraction patterns.” *Appl. Phys. Lett.* **107**, 183102 (2015).
- [6.18] Eisebitt, S. *et al.* “Lensless imaging of magnetic nanostructures by X-ray spectro-holography.” *Nature* **432**, 885–888 (2004).
- [6.19] Müller, G. M. *et al.* “Spin polarization in half-metals probed by femtosecond spin excitation.” *Nat. Mater.* **8**, 56–61 (2009).
- [6.20] Radu, I. *et al.* “Transient ferromagnetic-like state mediating ultrafast reversal of antiferromagnetically coupled spins.” *Nature* **472**, 205–208 (2011).
- [6.21] Ferrari, E. *et al.* “Widely tunable two-colour seeded free-electron laser source for resonant-pump resonant-probe magnetic scattering.” *Nat. Commun.* **7**, (2016).
- [6.22] Qi, X.-L. & Zhang, S.-C. “Topological insulators and superconductors.” *Rev. Mod. Phys.* **83**, 1057–1110 (2011).
- [6.23] Campi, G. *et al.* “Scanning micro-x-ray diffraction unveils the distribution of oxygen chain nanoscale puddles in  $\text{YBa}_2\text{Cu}_3\text{O}_{6.33}$ .” *Phys. Rev. B* **87**, 14517 (2013).

- [6.24] Edwards, H. L., Derro, D. J., Barr, A. L., Markert, J. T. & de Lozanne, A. L. "Spatially Varying Energy Gap in the CuO Chains of  $\text{YBa}_2\text{Cu}_3\text{O}_{7-x}$  Detected by Scanning Tunneling Spectroscopy." *Phys. Rev. Lett.* **75**, 1387–1390 (1995).
- [6.25] Lang, K. M. *et al.* "Imaging the granular structure of high-Tc superconductivity in underdoped  $\text{Bi}_2\text{Sr}_2\text{CaCu}_2\text{O}_{8+\delta}$ ." *Nature* **415**, 412–416 (2002).
- [6.26] Pan, S. H. *et al.* "Microscopic electronic inhomogeneity in the high-Tc superconductor  $\text{Bi}_2\text{Sr}_2\text{CaCu}_2\text{O}_{8+x}$ ." *Nature* **413**, 282–285 (2001).
- [6.27] Grübel, G., Stephenson, G. B., Gutt, C., Sinn, H. & Tschentscher, T. "XPCS at the European X-ray free electron laser facility." *Nucl. Instruments Methods Phys. Res. Sect. B Beam Interact. with Mater. Atoms* **262**, 357–367 (2007).
- [6.28] Fausti, D. *et al.* "Light-Induced Superconductivity in a Stripe-Ordered Cuprate." *Science* **331**, 189–191 (2011).
- [6.29] Khomskii, D. "Classifying multiferroics: Mechanisms and effects." *Physics (College Park, Md.)* **2**, 20 (2009).
- [6.30] Cheong, S.-W. & Mostovoy, M. "Multiferroics: a magnetic twist for ferroelectricity." *Nat. Mater.* **6**, 13–20 (2007).
- [6.31] Bibes, M. & Barthélémy, A. "Multiferroics: Towards a magnetoelectric memory." *Nat. Mater.* **7**, 425–426 (2008).
- [6.32] Kimura, T., Sekio, Y., Nakamura, H., Siegrist, T. & Ramirez, A. P. "Cupric oxide as an induced-multiferroic with high-Tc." *Nat. Mater.* **7**, 291–294 (2008).
- [6.33] Johnson, S. L. *et al.* "Femtosecond Dynamics of the Collinear-to-Spiral Antiferromagnetic Phase Transition in CuO." *Phys. Rev. Lett.* **108**, 37203 (2012).
- [6.34] Kida, N. *et al.* "Terahertz time-domain spectroscopy of electromagnons in multiferroic perovskite manganites." *JOSAB* **26(9)**, A35 (2009).
- [6.35] Mochizuki, M. & Nagaosa, N. "Theoretically Predicted Picosecond Optical Switching of Spin Chirality in Multiferroics." *Phys. Rev. Lett.* **105**, 147202 (2010).
- [6.36] Kubacka, T. *et al.* "Large-Amplitude Spin Dynamics Driven by a THz Pulse in Resonance with an Electromagnon." *Science* **343**, 1333–1336 (2014).
- [6.37] Leo, N. *et al.* "Polarization control at spin-driven ferroelectric domain walls." *Nat. Commun.* **6**, 6661 (2015).
- [6.38] Speedy, R. J. "Isothermal compressibility of supercooled water and evidence for a thermodynamic singularity at  $-45^\circ\text{C}$ ." *J. Chem. Phys.* **65**, 851 (1976).
- [6.39] Nilsson, A. & Pettersson, L. G. M. "The structural origin of anomalous properties of liquid water." *Nat. Commun.* **6**, 8998 (2015).
- [6.40] Stanley, H. E. & Mishima, O. "The relationship between liquid, supercooled and glassy water." *Nature* **396**, 329–335 (1998).
- [6.41] Poole, P. H., Sciortino, F., Essmann, U. & Stanley, H. E. "Phase behaviour of metastable water." *Nature* **360**, 324–328 (1992).
- [6.42] Amann-Winkel, K. *et al.* "Colloquium : Water's controversial glass transitions." *Rev. Mod. Phys.* **88**, 11002 (2016).
- [6.43] Wernet, P. *et al.* "The Structure of the First Coordination Shell in Liquid Water." *Science* **304**, (2004).
- [6.44] Tokushima, T. *et al.* "High resolution X-ray emission spectroscopy of liquid water: The observation of two structural motifs." *Chem. Phys. Lett.* **460**, 387–400 (2008).
- [6.45] Heigl, F., Lam, S., Regier, T., Coulthard, I. & Sham, T.-K. "Time-Resolved X-ray Excited Optical Luminescence from Tris(2-phenyl bipyridine)iridium." *J. Am. Chem. Soc.* **128**, 3906–3907 (2006).
- [6.46] Sham, T. K. *et al.* "Origin of luminescence from porous silicon deduced by synchrotron-light-induced optical luminescence." *Nature* **363**, 331–334 (1993).

- [6.47] Wallentin, J. *et al.* “InP Nanowire Array Solar Cells Achieving 13.8% Efficiency by Exceeding the Ray Optics Limit.” *Science* **339**, 1057–1060 (2013).
- [6.48] Mikkelsen, A. *et al.* “Direct imaging of the atomic structure inside a nanowire by scanning tunnelling microscopy.” *Nat. Mater.* **3**, 519–523 (2004).
- [6.49] Sham, T.-K. “Photon-In/Photon-Out Spectroscopic Techniques for Materials Analysis: Some Recent Developments.” *Adv. Mater.* **26**, 7896–7901 (2014).
- [6.50] Ulbricht, R., Hendry, E., Shan, J., Heinz, T. F. & Bonn, M. “Carrier dynamics in semiconductors studied with time-resolved terahertz spectroscopy.” *Rev. Mod. Phys.* **83**, 543–586 (2011).
- [6.51] Cocker, T. L. *et al.* “An ultrafast terahertz scanning tunnelling microscope.” *Nat. Photonics* **7**, 620–625 (2013).
- [6.52] Mårzell, E. *et al.* “Nanoscale Imaging of Local Few-Femtosecond Near-Field Dynamics within a Single Plasmonic Nanoantenna.” *Nano Lett.* **15**, 6601–6608 (2015).
- [6.53] Mårzell, E. *et al.* “Secondary electron imaging of nanostructures using Extreme Ultra-Violet attosecond pulse trains and Infra-Red femtosecond pulses.” *Ann. Phys.* **525**, 162–170 (2013).
- [6.54] Mikkelsen, A. *et al.* “Photoemission electron microscopy using extreme ultraviolet attosecond pulse trains.” *Rev. Sci. Instrum.* **80**, 123703 (2009).

# 7. Life Science

- *What makes us human?*
- *What is consciousness?*
- *Will we ever cure cancer?*
- *How do we beat multidrug-resistant bacteria?*

The scientific studies of living organisms is one of today's largest research areas that includes many of the big questions in science, like the ones above to just name a few. Many of these questions boil down to the structure and function of cells – the building blocks of life – including their internal cell organelles and other cellular components (see fig. 7.1). Below we review three scientific cases to study cells, proteins and other types of biomolecules using the ultrafast and ultrabright pulses of SXL.

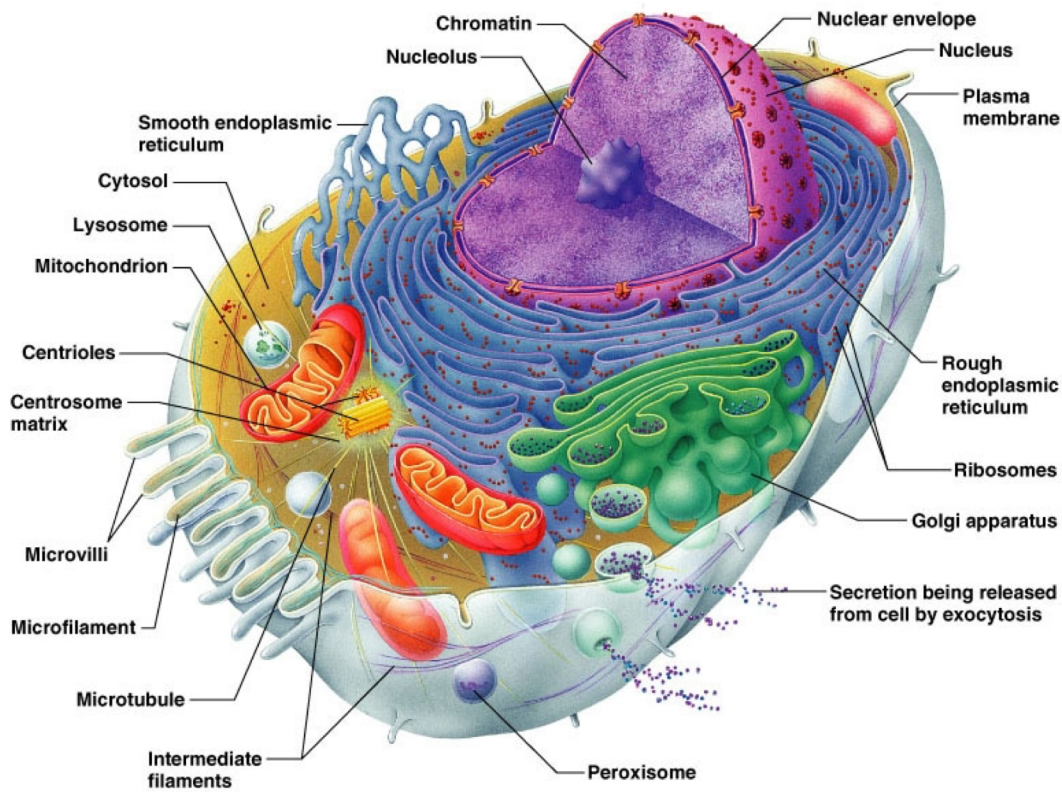


**Figure 7.1.** Schematic image of an eukaryotic cell with all cell organelles and other components labeled, visualizing the beauty and complexity of a cell's structure and function. (Reproduced from "Human Anatomy & Physiology" sixth edition, Elaine N. Marieb power point lecture. Copyright (2004) Pearson Education, Inc., publishing as Benjamin Cummings.)

## 7.1 Coherent diffractive imaging of living cells and other intrinsically heterogeneous biological building blocks

- *How does life organize itself inside cells on mesoscopic length scales?*
- *Can we observe rare events in living cells at nanoscale resolution using high-throughput coherent X-ray imaging?*

The scientific possibilities in life science was one of the main arguments to build the first hard X-ray FEL – the LCLS, *i.e.* to be able to record molecular movies of proteins, viruses and cells in their native state using coherent X-ray imaging. So far, the scientific output with biological impact has mostly been limited to protein nanocrystallography due to technical difficulties for X-ray imaging that has been limiting the resolution. Although the scattering signal from the rice dwarf virus of about  $\sim 70$  nm has repeatedly been measured out to  $\sim 6$  Å resolution [7.1], 2D reconstructions have been limited to  $\sim 30$  nm [7.2] for viruses,  $\sim 80$  nm [7.3] for cells and  $\sim 20$  nm [7.4] for cell organelles. 3D reconstructions require orienting many 2D diffraction patterns into a 3D intensity volume, which means that the sample has to be homogeneous and include highly reproducible particles. So far, only a few 3D reconstructions of biological particles have been made, including one of the Mimivirus that reached 125 nm resolution [7.5] (corresponding to  $\sim 10$  resolution elements), but with recent technical development several ongoing reconstructions of other viruses may reach a target resolution of 10-20 nm (corresponding to  $\sim 100$  resolution elements).

Although the 1 nm-wavelength of SXL limits the potential of studying individual biomolecules, the beamline will be well suited to perform coherent diffractive imaging of living cells (see fig. 7.2) and other large biological objects that are intrinsically heterogeneous with rare events that

require high throughput. Competing techniques such as cryo-electron microscopy cannot easily image whole cells of  $>1$   $\mu\text{m}$  at high resolution and especially not at high throughput, whereas optical light microscopy can achieve high resolution (2-25 nm) only for sparse subsets of photoactivatable fluorescent proteins through photoactivated localization microscopy (PALM) [7.6].

Another important point is that none of the competing techniques have the potential to image living cells at the nanoscale. A dose in excess of 100,000,000 Gray ( $\text{Gy} = \text{J kg}^{-1}$ ) would be required to reach nanometer resolution on a cell using X-rays or electrons [7.3], which no cell can survive. A dose of 20 Gy causes certain death in humans, 60–800 Gy kills most cells, and 25,000 Gy is lethal to all known organisms [7.7, 7.8]. As a result, X-ray microscopy and EM cryo-freeze samples have to be able to withstand the extreme radiation dose, whereas PALM requires thin cryo-sections of sample cut using an ultramicrotome [7.6]. The concept of diffraction before destruction [7.9] is thus opening new possibilities in life science to study living organisms at the nanoscale.

Good systems to develop live cell imaging at XFELs are cyanobacteria, since they are relatively small and play an important role in photosynthesis. They include the  $\text{O}_2$ -evolving complex Photosystem II in their thylakoid membranes and also contain bacterial polyhedral organelles known as carboxysomes that stand for 40% of Earth's carbon fixation [7.4]. The upper right part of fig. 7.2 shows a diffraction pattern of a single *synechococcus elongatus* cell with scattering signal recorded out to a resolution of  $\sim 4$  nm at a photon energy of 1100 eV. Although the scattered signal extends to a resolution 20 times higher than published 2D reconstructions of *cyanobium gracile* cells [7.3], the diffraction pattern could not be phased since it is saturated at the center part of the detector, thereby highlighting the challenging dynamic range that high-resolution cell imaging requires. The SXL

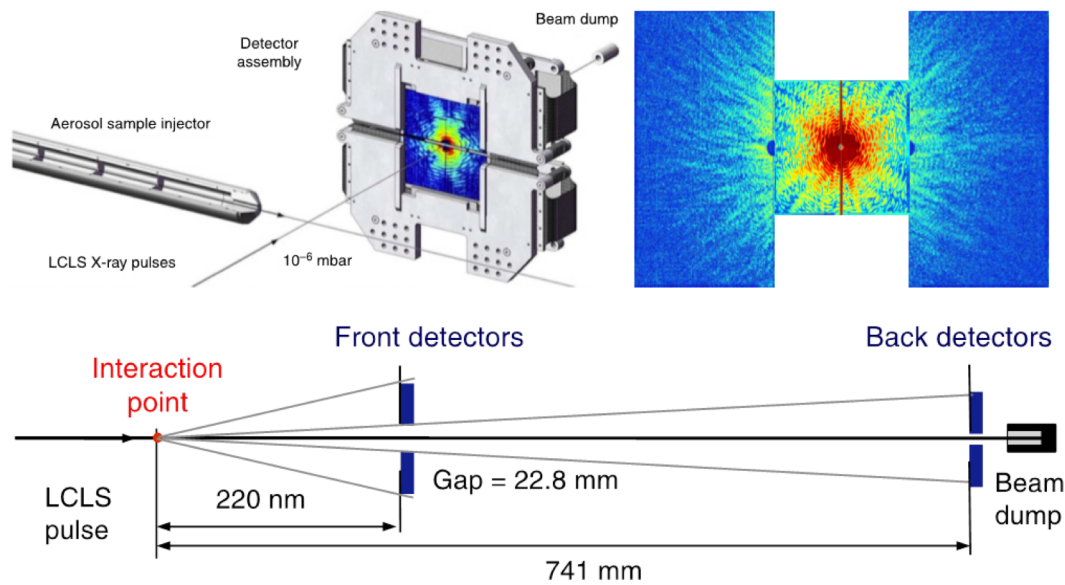


**Figure 7.2. Upper left:** Experimental setup of cyanobium gracile cells injected into  $10^{-6}$  mbar vacuum, intersected by ultrashort (fs) and ultrabright X-ray pulses produced by the LCLS and their diffraction pattern recorded on a pnCCD detector assembly. The direct beam passes through an opening in the center of the two detector halves. **Upper right:** Diffraction pattern of a single synechococcus elongatus cell with scattering signal recorded out to a resolution of  $\sim 4$  nm at a photon energy of 1100 eV (1.13 nm wavelength). **Bottom:** Geometrical arrangement of four pnCCD for high-resolution cell imaging. Each pnCCD has  $1024 \times 512$  pixels and an active area of  $76.8 \times 38.4$  mm<sup>2</sup>. (Upper left and bottom figures reprinted by permission from Macmillan Publishers Ltd: Nature. van der Schot, G. et al., Nat. Commun. **6**, 5704 (2015), copyright (2015). Upper right figure, unpublished.)

beamline could overcome these challenges with smart experimental design and state-of-the-art detectors.

## 7.2 Fluctuation-based X-ray scattering of conformational changes in protein solutions

- Can we observe light-stimulated, fast conformational changes in protein solutions?
- How do phytochrome photosensors connect to the cellular signaling network so that they can control diverse cellular functions?
- What is the mechanism of protein folding that renders it possible to navigate on the energy landscape of proteins to form the native state?

The technical challenges of single-particle imaging become severe when nanoscale objects with low scattering cross section ought to be recorded over a high range of momentum transfer  $q$  to achieve high resolution. One way to circumvent the inherently low scattering cross section of a single protein is to measure an ensemble of proteins in solution, which can be done in conventional small-angle X-ray scattering (SAXS) and wide-angle X-ray scattering (WAXS). The downside of SAXS and WAXS is that the intensity in the 2D pattern is limited to 1D information content as function of  $q$ . A theory has been developed [7.10-7.13] to increase the information content in SAXS and WAXS by analyzing angular correlations in the fluctuations of the isotropic scattering pattern of a liquid or solution, which extends the information content from pair correlations to include pair correlations as well as triple correlations. In 2D-like systems

randomly oriented about a single axis parallel with the X-ray beam [7.14] and 3D systems with cylindrical symmetry [7.15], the information content is sufficient to reconstruct the particle density *ab initio*. In a 3D system with a randomly oriented particle, the information content is not sufficient to reconstruct the full 3D structure *ab initio*, but is expected to be  $\sim 10$  times larger than that of 1D SAXS and can be used together with a priori knowledge to refine a model. Experimental

results have so far been achieved for colloidal samples [7.16] and metal nanoparticles [7.14, 7.17], whereas useful information has not been obtained for molecular systems at atomic distances (*i.e.* WAXS regime). This is due to the experimental challenges to detect fluctuations that scale as  $\sqrt{N}$  compared to the isotropic scattering signal that scales linearly with number of particles  $N$ .

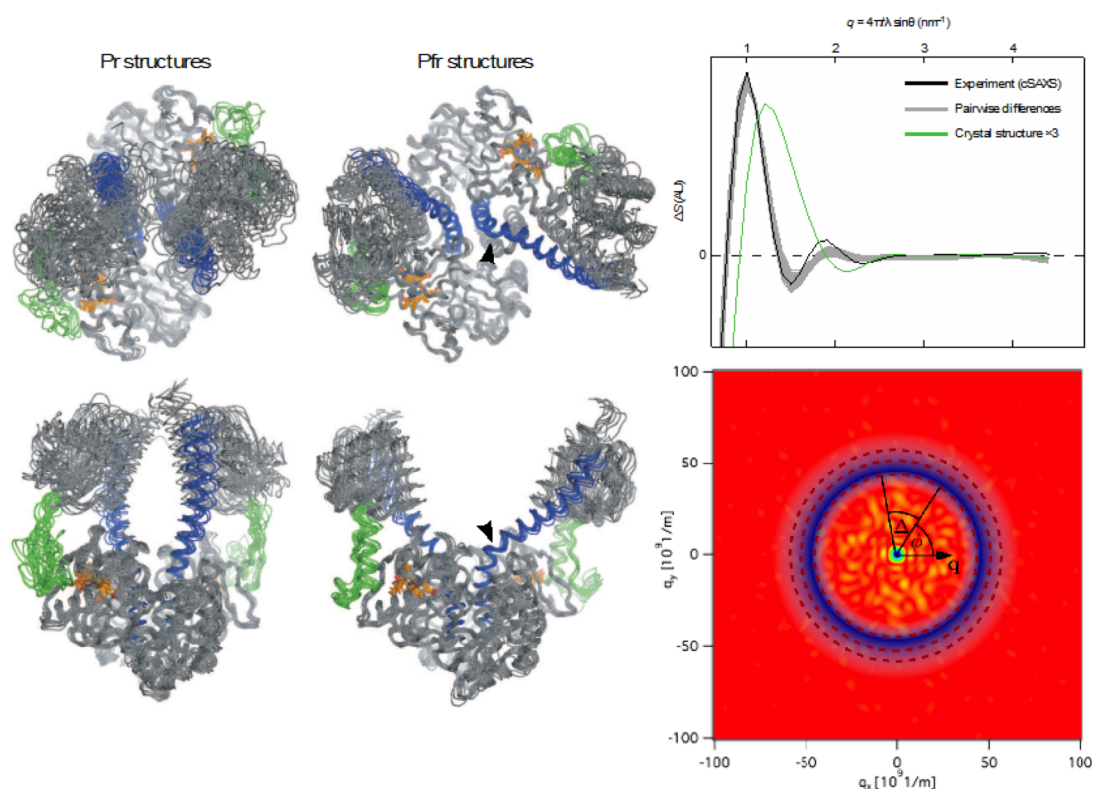


**Figure 7.3.** *Left:* Representative solution structures for red-absorbing (Pr) and far-red-absorbing (Pfr) states of the photosensory core in phytochromes from *deinococcus radiodurans*, identified from solution SAXS. *Upper right:* Solution difference SAXS between the proposed solution structures (Pfr – Pr, grey) compared to experimental SAXS data (black) and difference scattering calculated from crystal structures (green). *Lower right:* Angular correlations in fluctuation-based SAXS will increase the information content compared to conventional SAXS and also include triple correlations in addition to pair correlations. (Left and upper right figures reprinted by permission from Macmillan Publishers Ltd: Nature. Takala, H. et al., Nature **509**, 245-248 (2014), copyright (2014). Lower right, figure, unpublished.)

Despite the technical difficulties, fluctuation-based X-ray scattering has the potential to observe conformational changes in large ensembles of proteins in solution, since the signal-to-noise ratio is expected to be independent of  $N$  above  $\sim 10$  particles [7.18]. The ultrashort and ultrabright pulses at SXL would freeze all molecular motion and the instantaneous scattering as a snapshot of the solution could be used to extract information beyond conventional 1D SAXS. A good system as proof of concept would be phytochrome photosensors (see fig. 7.3) – a family of red-light-sensing kinases that control diverse cellular functions in plants [7.19], bacteria [7.20] and fungi [7.21] – for which a conformational change of several nanometers occurs reversibly upon optical laser excitation [7.22]. The structural change is controlled by refolding of an evolutionarily conserved P-R-X-S-F motif in the dimeric protein that results in a 2.5 Å change, which eventually grows into a nanoscale conformational signal [7.22]. Time-resolved fluctuation-based SAXS at the SXL beamline could shine further light upon the mechanism with which the phytochromes connect to the cellular signaling network.

### 7.3 Energy conversion involving non-adiabatic dynamics probed by ultrafast X-ray spectroscopy

- *What is the mechanism behind non-adiabatic dynamics that allow for very fast, efficient and selective energy transfer channels?*
- *Can we understand Nature's photoprotection mechanisms?*

Nature is rich in efficient and economic molecular machines, like the opsin shown in fig. 7.4 (left), that master the challenge of transforming light energy from the sun selectively into altered bonds or separated charges. Nature also has prepared protection mechanisms for precious molecules that allow dissipation of excess energy into heat. The common approach to simplify molecular dynamics is the Born-Oppenheimer approximation (BOA) allowing for the separation of electronic and nuclear degrees of freedom [7.23]. Over the recent two decades ultrafast spectroscopy has discovered the breakdown of the BOA in many important optically excited molecules, as for instance in so-called conical intersections (indicated by the grey cones in fig. 7.4 (right)). Non-BOA physics allows for very fast and thus very efficient and selective energy transfer channels [7.24-7.26].

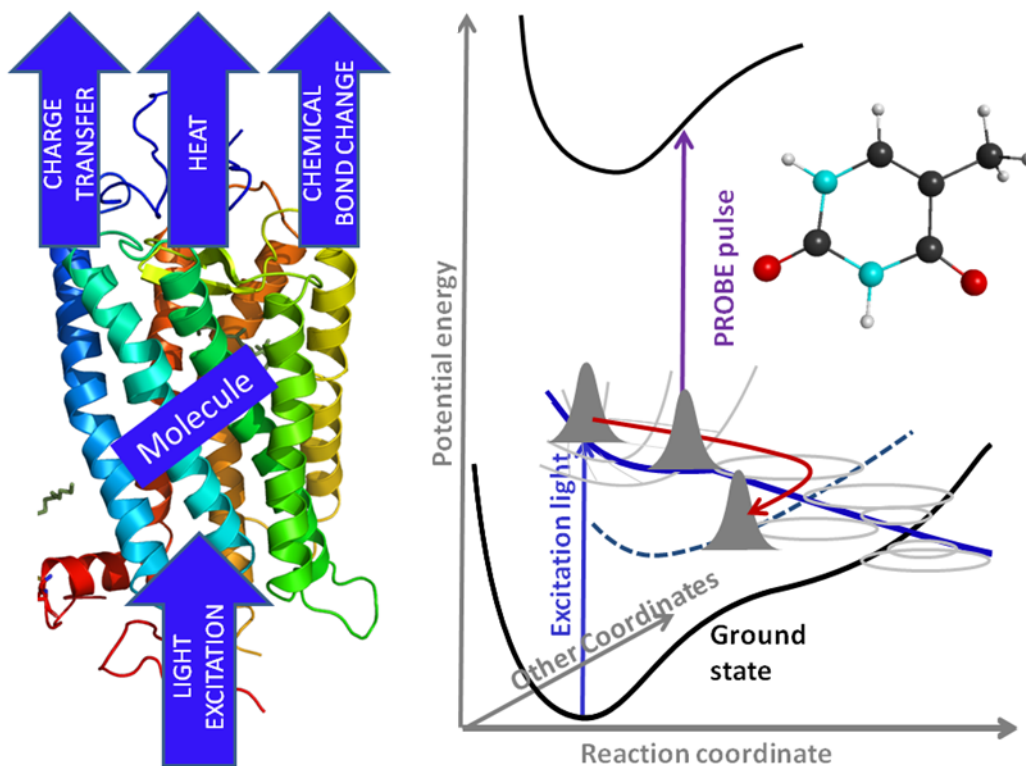


**Figure 7.4.** *Left:* Molecules are highly selective systems that convert light energy into other energetic forms such as changes in chemical bonds, heat or charge separation. (Figure modified based on Ref. [7.27].) **Right:** Potential energy representation of light conversion and ultrafast probing (for a nucleobase). Light (in form of a short pulse) excites molecules from the ground electronic state to a valence-excited state (blue). To counteract photoinduced reactions, the electronic energy is funneled into a lower lying  $n\pi^*$  state via non-adiabatic dynamics, as given by the red arrow. (Reprinted by permission from M. Guehr, Potsdam University.)

The DNA in our skin is continuously exposed to light, and the ultraviolet spectral region contains sufficient photon energy to damage DNA by either breaking the DNA double strand or by fragmenting the nucleobases. To avoid photochemical decomposition, the nucleobases have ultrafast pathways for funneling the population from the excited electronic state down

into the ground state via non-adiabatic dynamics. An example of this mechanism for the nucleobase thymine is shown in fig. 7.4 (right). The interpretation of the transient states is complicated, and the relaxation from the excited state to the ground state may only be possible with a violation of the Born-Oppenheimer approximation.

## References

- [7.1] Munke, A. *et al.* “Coherent diffraction of single Rice Dwarf virus particles using hard X-rays at the Linac Coherent Light Source.” *Sci. Data* **3**, 160064 (2016).
- [7.2] Seibert, M. M. *et al.* „Single mimivirus particles intercepted and imaged with an X-ray laser.” *Nature* **470**, 78–81 (2011).
- [7.3] van der Schot, G. *et al.* „Imaging single cells in a beam of live cyanobacteria with an X-ray laser.” *Nat. Commun.* **6**, 5704 (2015).
- [7.4] Hantke, M. F. *et al.* ”High-throughput imaging of heterogeneous cell organelles with an X-ray laser.” *Nat. Photonics* **8**, 943–949 (2014).
- [7.5] Ekeberg, T. *et al.* “Three-Dimensional Reconstruction of the Giant Mimivirus Particle with an X-Ray Free-Electron Laser.” *Phys. Rev. Lett.* **114**, 98102 (2015).
- [7.6] Betzig, E. *et al.* “Imaging Intracellular Fluorescent Proteins at Nanometer Resolution.” *Science* **313**, 1642–1645 (2006).
- [7.7] Fairand, B. P. “Radiation sterilization for health care products : x-ray, gamma, and electron beam.” (CRC Press, 2002).
- [7.8] Game, J. C., Williamson, M. S. & Baccari, C. “X-ray survival characteristics and genetic analysis for nine *Saccharomyces* deletion mutants that show altered radiation sensitivity.” *Genetics* **169**, 51–63 (2005).
- [7.9] Chapman, H. N. *et al.* ”Femtosecond diffractive imaging with a soft-X-ray free-electron laser.” *Nat. Phys.* **2**, 839–843 (2006).
- [7.10] Kam, Z. “Determination of Macromolecular Structure in Solution by Spatial Correlation of Scattering Fluctuations.” *Macromolecules* **10**, 927–934 (1977).
- [7.11] Kam, Z., Koch, M. H. & Bordas, J. “Fluctuation x-ray scattering from biological particles in frozen solution by using synchrotron radiation.” *Proc. Natl. Acad. Sci. U. S. A.* **78**, 3559–62 (1981).
- [7.12] Altarelli, M., Kurta, R. P. & Vartanyants, I. A. “X-ray cross-correlation analysis and local symmetries of disordered systems: General theory.” *Phys. Rev. B* **82**, 104207 (2010).
- [7.13] Kurta, R. P., Altarelli, M., Weckert, E. & Vartanyants, I. A. “X-ray cross-correlation analysis applied to disordered two-dimensional systems.” *Phys. Rev. B* **85**, 184204 (2012).
- [7.14] Saldin, D. K. *et al.* ”New Light on Disordered Ensembles: *Ab Initio* Structure Determination of One Particle from Scattering Fluctuations of Many Copies.” *Phys. Rev. Lett.* **106**, 115501 (2011).
- [7.15] Starodub, D. *et al.* “Single-particle structure determination by correlations of snapshot X-ray diffraction patterns.” *Nat. Commun.* **3**, 1276 (2012).
- [7.16] Wochner, P. *et al.* “X-ray cross correlation analysis uncovers hidden local symmetries in disordered matter.” *Proc. Natl. Acad. Sci. U. S. A.* **106**, 11511–4 (2009).
- [7.17] Mendez, D. *et al.* “Observation of correlated X-ray scattering at atomic resolution.” *Philos. Trans. R. Soc. B Biol. Sci.* **369**, 20130315–20130315 (2014).
- [7.18] Kirian, R. A., Schmidt, K. E., Wang, X., Doak, R. B. & Spence, J. C. H. “Signal, noise, and resolution in correlated fluctuations from snapshot small-angle x-ray scattering.” *Phys. Rev. E* **84**, 11921 (2011).
- [7.19] Butler, W. L., Norris, K. H., Siegelman, H. W. & Hendricks, S. B. “Detection, Assay, and Preliminary Purification of the Pigment Controlling Photoresponsive Development of Plants.” *Proc. Natl. Acad. Sci. U. S. A.* **45**, 1703–8 (1959).

- [7.20] Yeh, K. C., Wu, S. H., Murphy, J. T. & Lagarias, J. C. "A cyanobacterial phytochrome two-component light sensory system." *Science* **277**, 1505–8 (1997).
- [7.21] Blumenstein, A. *et al.* "The *Aspergillus nidulans* Phytochrome FphA Represses Sexual Development in Red Light." *Curr. Biol.* **15**, 1833–1838 (2005).
- [7.22] Takala, H. *et al.* "Signal amplification and transduction in phytochrome photosensors." *Nature* **509**, 245–8 (2014).
- [7.23] Canton, S. E. *et al.* "Visualizing the non-equilibrium dynamics of photoinduced intramolecular electron transfer with femtosecond X-ray pulses." *Nat. Commun.* **6**, 6359 (2015).
- [7.24] Wernet, P. *et al.* "Orbital-specific mapping of the ligand exchange dynamics of Fe(CO)<sub>5</sub> in solution." *Nature* **520**, 78–81 (2015).
- [7.25] Harlang, T. C. B. *et al.* "Iron sensitizer converts light to electrons with 92% yield." *Nat. Chem.* **7**, 883–889 (2015).
- [7.26] George, C., Ammann, M., D'Anna, B., Donaldson, D. J. & Nizkorodov, S. A. "Heterogeneous Photochemistry in the Atmosphere." *Chem. Rev.* **115**, 4218–4258 (2015).
- [7.27] [https://de.wikipedia.org/wiki/Rhodopsin#/media/File:1L9H\\_\(Bovine\\_Rhodopsin\)\\_2.png](https://de.wikipedia.org/wiki/Rhodopsin#/media/File:1L9H_(Bovine_Rhodopsin)_2.png)

# 8. Theory Support for New Experiments

---

- *Can we develop suitable computational techniques that support the SXL-experiments?*
- *Can we develop theoretical methods, which specifically target RIXS-measurements, nonlinear X-ray processes, electron dynamics, and molecular as well as solid state properties?*

In order to increase beamline productivity and to stimulate the process of scientific discovery, a concomitant investment in development of theory and simulation techniques is called for. It is of particular importance that young theoreticians in X-ray sciences are trained to support the sizable investments on the experimental side. To this end an active collaboration between the seven leading theory groups in Sweden has been established with support from the Knut and Alice Wallenberg foundation (KAW). A strong focus is put on developing and extending computational techniques and programs which can be applied to analyze and interpret data from experimental studies of, for example, new materials, biomolecules in relevant environments, correlated materials, magnetism, heterogeneous catalysis, and the properties of liquids and solutions. This theory consortium is already well poised to provide strong support to future SXL experiments.

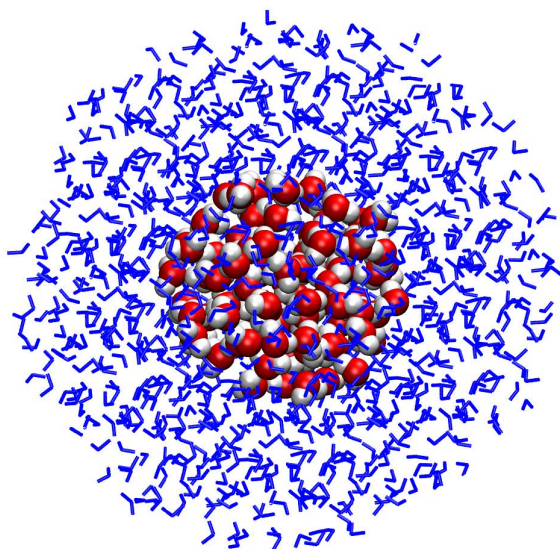
## 8.1 Methods development

Our main focus for the development of computational approaches to address RIXS and multi-photon X-ray processes which are important for SXL, is to extend the complex polarization propagator (CPP) method to the nonlinear case and to fully incorporate a molecular mechanics (MM) description of the environment. We aim to develop the theory for RIXS both for photon-out (radiative RIXS) and electron-out (resonant photo-emission) experiments. With this we complete the QM/MM

(Quantum mechanics/MM) treatment of the whole family of X-ray spectroscopies, which is open-ended for further development in terms of improved reference state electronic structure models, higher-order propagators, as well as for the QM/MM methodology itself.

The QM/MM approach has recently been extensively tested by computing X-ray absorption spectra of liquid water and ice using both transition-potential density functional (TP-DFT) and CPP techniques with and without the MM embedding [8.1]. It was demonstrated that spectra of unprecedented quality for liquid water and ice could be obtained with the CPP/DFT technique in conjunction with a mix of a QM and MM description of the environment. Such a mix is illustrated in fig. 8.1 where we compute spectra for a model of liquid water using a central 96 molecules cluster which is then embedded in an environment consisting of 1007 molecules described at the simplified MM level.

In a semi-classical framework, the response function describing the linear absorption cross section due to an exact linearly polarized electromagnetic field has been derived and implemented in the CPP/DFT framework [8.2]. The formulation is based on the full field-matter interaction operator and is gauge-origin invariant also with use of incomplete basis sets. The derivation and implementation of the second-order nonlinear CPP response function has recently been made at the DFT level. It enables calculations of the imaginary part of the response function governing the intensity dependent refractive index which describes the two-photon absorption (TPA) cross section. The first *ab initio*



**96 QM + 1007 MM**

**Figure 8.1.** Illustration of a mix of QM and MM descriptions of the environment using a central 96 molecules cluster embedded in 1007 molecules described at the simplified MM level.

calculations of X-ray TPA (XTPA) have been performed [8.3]. This work opens up the field for theoretical nonlinear X-ray spectroscopies as it forms an essential corner stone for the development of the nonlinear response functions needed to describe RIXS and other nonlinear X-ray processes that will be important at SXL.

Advanced time-dependent wave-packet techniques have been developed which can describe coupled electron nuclear dynamics as observed in enhanced one-photon two-electron transitions in RIXS of CO [8.4]. Multidimensional wave packet theory has been

developed which allows reproducing and explaining the formation of vibrational features in resonant X-ray scattering transitions via dissociative and bound core-excited states in gaseous water. In the strong X-ray field regime, relevant for SXL, stimulated emission processes in diatomic molecules can now be studied [8.5]. The time-dependent density functional theory (TDDFT) method has been extended to calculate X-ray photoelectron spectroscopy (XPS) shake-up satellites at organic-metal interfaces. The multi-configurational self-consistent field (MCSCF) approach has been extended to simulate attosecond optical-X-ray pump-probe spectroscopy and all-X-ray double-quantum coherence spectroscopy. The former allows monitoring electron dynamics near conical intersections, and the latter is found to be very sensitive to isomerization and intramolecular charge transfer properties.

The above developments are related to molecular properties, but members of the consortium have also completed several technical developments and improvements of condensed phase approaches. In particular, regarding the full-potential, all-electron, electronic structure method which can handle strongly correlated electron systems like transition metal oxides, *e.g.* cuprate superconductors as demonstrated in the study on the magnetic and spectral properties of Tb clusters [8.6]. Other research efforts concern polaritonic states that form under intense light interactions with electron states of a material. Zitterbewegung in graphene has been found [8.7] to result from such effects.

## XAS of NiO

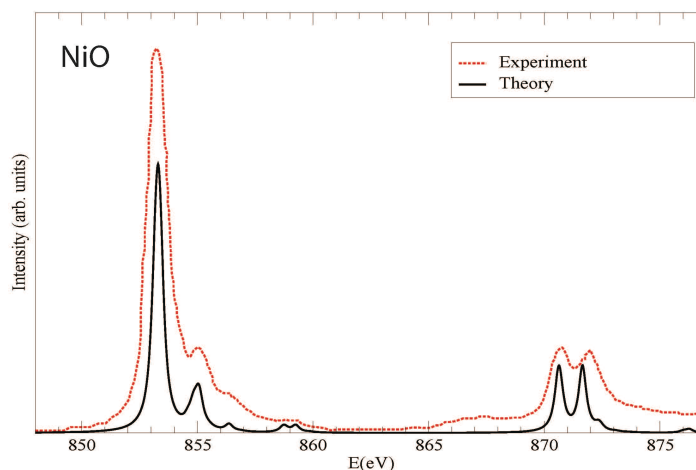


**Figure 8.2.** Comparison of experimental and theoretical L-edge X-ray absorption spectra for NiO [8.8].

The accuracy of solid-state electronic structure methods was recently investigated systematically [8.9]. Here it was found that modern electronic structure theories give results that in all practical aspects are identical. Transition metal L-edge X-ray spectra can be accurately simulated ab initio without symmetry constraints through independent development in

the solid state framework and molecular quantum chemistry [8.10, 8.11]. This sets a basic foundation for further developments of these methods for calculating theoretical spectra. An example of this is shown in fig. 8.2 where the theoretical X-ray absorption spectrum of NiO is compared to experimental data.

## References

- [8.1] Fransson, T. *et al.* “Requirements of first-principles calculations of X-ray absorption spectra of liquid water.” *Phys. Chem. Chem. Phys.* **18**, 566–583 (2016).
- [8.2] List, N. H., Kauczor, J., Saue, T., Jensen, H. J. A. & Norman, P. “Beyond the electric-dipole approximation: A formulation and implementation of molecular response theory for the description of absorption of electromagnetic field radiation.” *J. Chem. Phys.* **142**, 244111 (2015).
- [8.3] Fahleson, T., Ågren, H. & Norman, P. “A Polarization Propagator for Nonlinear X-ray Spectroscopies.” *J. Phys. Chem. Lett.* **7**, 1991–1995 (2016).
- [8.4] Couto, R. C. *et al.* “Anomalously strong two-electron one-photon X-ray decay transitions in CO caused by avoided crossing.” *Sci. Rep.* **6**, 20947 (2016).
- [8.5] Kimberg, V. & Rohringer, N. “Stochastic stimulated electronic x-ray Raman spectroscopy.” *Struct. Dyn.* **3**, 34101 (2016).
- [8.6] Peters, L. *et al.* “Magnetism and exchange interaction of small rare-earth clusters; Tb as a representative.” *Sci. Rep.* **6**, 19676 (2016).
- [8.7] Yudin, D., Eriksson, O. & Katsnelson, M. I. “Dynamics of quasiparticles in graphene under intense circularly polarized light.” *Phys. Rev. B* **91**, 75419 (2015).
- [8.8] Lueder *et al.* Unpublished.
- [8.9] Lejaeghere, K. *et al.* “Reproducibility in density functional theory calculations of solids.” *Science* **351**, 1415 (2016).
- [8.10] Haverkort, M. W., Zwierzycki, M. & Andersen, O. K. “Multiplet ligand-field theory using Wannier orbitals.” *Phys. Rev. B* **85**, 165113 (2012).
- [8.11] Josefsson, I. *et al.* “Ab Initio Calculations of X-ray Spectra: Atomic Multiplet and Molecular Orbital Effects in a Multiconfigurational SCF Approach to the L-Edge Spectra of Transition Metal Complexes.” *J. Phys. Chem. Lett.* **3**, 3565–3570 (2012).

# Appendix

## A. The SXL Workshop

### A.1 Pictures



*Workshop participants in the The Svedberg Hall.*



*Group picture of workshop participants.*



*Presentation by Per Johnsson.*



*Ingolf Lindau, Wilfried Wurth and Robert Schoenlein.*



*Seminar in the Oscar Klein Auditorium.*



*Picture from the chemistry breakout session.*

## A.2 Program

### MONDAY, MARCH 21

09:00 – 10:00	Registration		
10:00 – 11:00	Introduction to the meeting, Room: F05 Chair: <i>Anders Nilsson</i> (Workshop logistics) <i>Anders Karlhede</i> (Deputy Vice-Chancellor for Science, Stockholm University) <i>Mats Larsson</i> (Director of the Stockholm-Uppsala Center for Free Electron Laser Research) <i>Jejper Andersen</i> (Science Director at MAX IV Laboratory) <i>Sverker Werlin</i> (Possible outlines of SXL at MAX IV)		
11:00 – 11:30	Plenary session, Room: F05 Chair: <i>Anders Nilsson</i>		
11:30 – 12:00	FEL Research and Development at the LCLS, <i>Zhirong Huang</i>		
12:00 – 12:15	Control of soft X-ray pulses at the seeded Free Electron Laser FERMI, <i>Enrico Allaria</i>		
12:15 – 12:30	Lund Laser Centre, <i>Per Johnsson</i>		
12:30 – 13:30	Opportunities for THz pump / x-ray probe investigations at SXL, <i>Stefano Bonetti</i>		
	LUNCH		
13:30 – 14:00	Room: F042 Chair: <i>Michael Odellius</i>	Room: F05 Chair: <i>Oscar Ternberg</i>	Room: F041 Chair: <i>Jan-Erik Rubensson</i>
14:00 – 14:30	Probing photochemistry of isolated molecules by short x-ray pulses, <i>Marcus Göhr</i>	Probing the dynamics of electronic orderings using time-resolved resonant x-ray scattering, <i>Yr-De Chuang</i>	Multi-Wave Mixing at FERMI, <i>Claudio Masciocchio</i>
14:30 – 15:00	Probing ultrafast surface chemistry and catalysis with optical and soft x-ray lasers, <i>Henrik Gustaf</i>	Quenching of the Resonant Short Free-Electron Laser Light Pulses, <i>Magnus Bernsten</i>	Stimulated x-ray Raman scattering in molecules, <i>Victor Kimberg</i>
15:00 – 15:30	Opportunity to probe oxidation-reduction (redox) reactions at interfaces using SXL, <i>Hiroto Ogawara</i>	Experiments for stimulated soft X-ray emission from solids, <i>Martin Beye</i>	Towards controlled manipulation of inner-shell electrons, <i>Linda Young</i>
	COFFEE BREAK		
15:30 – 16:00	Room: F042 Chair: <i>Michael Odellius</i>	Room: F05 Chair: <i>Oscar Ternberg</i>	Room: F041 Chair: <i>Per Johnsson</i>
16:00 – 16:30	Localization of electrons with x-rays: prospects and challenges, <i>Dennis Nordlund</i>	Controlling Resonant Soft X-Ray Processes through Stimulation, <i>Jocelyn Stohr</i>	Towards a complete picture of few X-ray photons driven ionization, <i>Raimund Feifel</i>
16:30 – 17:00	Femtosecond X-ray Spectroscopy for photochemicals, <i>Martina Dell’Angelo</i>	Resonant Magnetic Scattering, <i>Gerhard Grübel</i>	Resonant and non-resonant multi-photon processes in atoms, <i>Michael Meyer</i>
	BREAKOUT SESSIONS (See details below)		
17:00 – 18:00	BREAKOUT SESSIONS (AMOs: F041, Chemistry: F042, Condensed Matter: FA32, FEL Science: A3:1003, Life Sciences: F041, Novel Spectroscopy: FA31)		
18:00 – 20:00	RECEPTION		

### TUESDAY, MARCH 22

09:00 – 09:30	Room: F042 Chair: <i>Henrik Gustaf</i>	Room: F052 Chair: <i>Stefano Bonetti</i>	Room: F055 Chair: <i>Richard Meuze</i>
10:00 – 10:30	Electronic and Structural Dynamics in Metal Complexes enlightened by XFEL Experiments, <i>Martin Medford Nielsen</i>	Femtosecond dynamics of antiferromagnetic spin order in an induced multiferroic, <i>Steve Johnson</i>	Coherent diffractive imaging of giant amoeba viruses, <i>Jonas Selberg</i>
10:30 – 11:00	Medford Nielsen	Towards controlling spins in space and time, <i>Hermann Dürr</i>	Single particle imaging: the past and the future, <i>Filipe Maia</i>
11:00 – 13:00	Dynamics of electrons at work in solar energy conversion, <i>Villy Sundström</i>	Seeing Spins Move, <i>Stefan Eisehitt</i>	1D crystallography: XFEL imaging of biological assemblies with helical symmetry, <i>Gisela Brändén</i>
	COFFEE BREAK		
	BREAKOUT SESSIONS AMOs: F041 Chemistry: F042 Condensed Matter: F052 FEL Science: F051 Life Sciences: F041 Novel Spectroscopy: F055		
	LUNCH		
14:00 – 14:30	Plenary session, Room: F05 Chair: <i>Mats Larsson</i>		
14:30 – 15:00	Science Opportunities for the LCLS-II High Repetition Rate Soft X-ray Laser, <i>Robert Schoenlein</i>		
15:00 – 15:30	Experimental strategies and research perspectives taking advantage of fully coherent EUV-Soft X-ray FERMI radiation, <i>Magnus Kiskinow</i>		
15:30 – 16:00	Soft x-ray science opportunities and instrumentation at European XFEL, <i>Andreas Schierz</i>		
16:00 – 17:30	COFFEE BREAK		
	Plenary Session, Room: F05 Chair: <i>Anders Nilsson</i>		
	BREAKOUT SESSIONS SUMMARY (15 minutes/group)		

Continued on next page... →

**WEDNESDAY, MARCH 23**

**Plenary session, Room: FDS**

*Chair: Mats Larsson*

09:00 – 09:30 FLASH - a High Repetition Rate XUV and Soft X-Ray FEL, *Wilfried Wurth*  
09:30 – 10:00 SwissFEL: expanding capabilities with ATHOS, *Rafael Abela*

**10:00 – 10:30**

**COFFEE BREAK**

**10:30 – 12:00**

**BREAKOUT SESSIONS**

AMMO: FB41  
Chemistry: FB42  
Condensed Matter: FB52  
FEL Science: FB55  
Life Sciences: FD41  
Novel Spectroscopy: FB51

**12:00 – 13:00**

**LUNCH**

**13:00 – 14:30**

**Plenary Session, Room: FDS**

*Chair: Anders Nilsson*

**BREAKOUT SESSIONS SUMMARY (15 minutes/group)**

**14:30 – 14:55**

Summary of the meeting, *Ingolf Lindau*

**14:55 – 15:00**

End of meeting, *Anders Nilsson*



### A.3 Participants

Dr. ABELA, Rafael	Paul Scherrer Institut	Switzerland
ABERGEL, David	Nordita	Sweden
Dr. AFANEH, Feras	Physics Department, Hashemite University	Jordan
ALLARIA, Enrico	Elettra - Sincrotrone Trieste	Italy
Dr. ALLGARDSSON, Anders	Swedish Defence Research Agency, FOI	Sweden
Dr. AMANN-WINKEL, Katrin	Stockholm University / Fysikum	Sweden
Dr. AMANN, Peter	Stockholm University / Fysikum	Sweden
Prof. ANDERSEN, Jesper	MAX IV Laboratory	Sweden
Dr. BERNTSEN, Magnus H.	KTH Royal Institute of Technology	Sweden
Ms. BESHARAT, zahra	KTH	Sweden
Dr. BEYE, Martin	Helmholtz-Zentrum Berlin	Germany
Prof. BJÖRNEHOLM, Olle	Department of Physics and Astronomy	Sweden
Dr. BONETTI, Stefano	Stockholm University	Sweden
BRÄNDÉN, Gisela	University of Gothenburg	Sweden
Dr. BURZA, Matthias	Max IV Laboratoriet	Sweden
BÖRJESSON, Lars	Chalmers	Sweden
Dr. CALEMAN, Carl	Uppsala University, Dept. of Physics and Astronomy	Sweden
CALLEGARI, Carlo	Elettra Sincrotrone Trieste	Italy
CHEN, Hong	Organic Chemistry, KTH	Sweden
Dr. CHUANG, Yi-De	Lawrence Berkeley National Laboratory	United States
Dr. CORENO, Marcello	CNR-ISM and Elettra	Italy
Mr. COUTO, Rafael	KTH	Sweden
CURBIS, Francesca	MAX IV Laboratory	Sweden
Dr. DAHLSTRÖM, Jan Marcus	Stockholm Univeristy	Sweden
Mr. DEGERMAN, David	Chemical Physics	Sweden
Dr. DELL'ANGELA, Martina	CNR-IOM Istituto Officina dei Materiali	Italy
Prof. DURR, Hermann	SLAC National Accelerator Laboratory	United States
Prof. EISEBITT, Stefan	Max-Born-Institut	Germany
Dr. ENQUIST, Henrik	MAX IV Laboratory	Sweden
Prof. FEIFEL, Raimund	Department of Physics	Sweden
FERNANDES TAVARES, Pedro	MAX IV Laboratory	Sweden
Ms. FOGELQVIST, Emelie	Applied Physics	Sweden
Prof. FÖHLISCH, Alexander	Inst. for Methods and Instr. in Synchrotron Rad. Research	Germany
GELMUKHANOV, Faris	KTH	Sweden
Ms. GENG, Ting	Stockholm University	Sweden
Mr. GHADAMI YAZDI, Milad	Material Physics, KTH	Sweden
Dr. GORYASHKO, Vitaliy	Uppsala University	Sweden
Ms. GRAY, Amber	Blekinge Institute of Technology	Sweden
Mr. GRAZIOLI, Cesare	University of Trieste, Dept. of Chem. and Pharm. Sciences	Italy
Prof. GRUEBEL, Gerhard	DESY, Hamburg	Germany
GUEHR, Markus	Potsdam University	Germany
Prof. GÖTHELID, Mats	Materialfysik	Sweden
HAMBERG, Mathias	Uppsala University	Sweden

Mr. HAMMARIN, Greger	Biochemistry and Biophysics, Gothenburg university	Sweden
Prof. HANSSON, Tony	Fysikum	Sweden
HEDBERG, Claes	Blekinge Tekniska Högskolan	Sweden
Dr. HELLSVIK, Johan	KTH, Department of Materials and Nano Physics	Sweden
Prof. HUANG, Zhirong	SLAC	United States
Dr. HUA, Weijie	KTH	Sweden
Dr. HUDL, Matthias	Stockholm University	Sweden
Prof. HUTTULA, Marko	University of Oulu	Finland
Prof. JOHNSON, Steven	ETH Zurich	Switzerland
Dr. JOHNSON, Per	Lund University	Sweden
Dr. JURICIC, Vladimir	Nordita, Nordic Institute for Theoretical Physics	Sweden
Prof. KANSKI, Janusz	CTH	Sweden
KARLHEDE, Anders	Stockholm University	Sweden
Dr. KIMBERG, Victor	Royal Institute of Technology	Sweden
Dr. KIM, Kyung Hwan	Department of Physics, Stockholm University	Sweden
Dr. KISKINOVA, Maya	Elettra Sincrotrone Trieste	Italy
KLOO, Lars	KTH	Sweden
Dr. KNOPP, Gregor	Paul Scherrer Institute	Switzerland
Dr. KULYK, Kostiantyn	Stockholm University	Sweden
Mr. KÖRDEL, Mikael	Biox, Applied Physics, KTH	Sweden
Dr. LARSSON, Daniel	Uppsala University	Sweden
Mr. LARSSON, Jakob	KTH	Sweden
Prof. LARSSON, Jörgen	Lund University	Sweden
Prof. LARSSON, Mats	Department of Physics, Stockholm University	Sweden
Prof. LINDAU, Ingolf	SLAC, Stanford	United States
Prof. LINDROTH, Eva	Department of Physics, Stockholm University	Sweden
Dr. LIU, Xianjie	Linköping University	Sweden
Dr. LUNDH, Olle	Lund University	Sweden
Mr. LUNDQVIST, Tomas	MAX IV Laboratory	Sweden
MAIA, Filipe	Uppsala University	Sweden
MANNIX, Danny	Department of Physics Lund University	Sweden
Prof. MARKLUND, Mattias	Department of Physics	Sweden
MARKS, Kess	Stockholm University	Sweden
Dr. MASCIOVECCHIO, Claudio	Elettra Sincrotrone Trieste	Italy
MEEDOM NIELSEN, Martin	Technical University of Denmark	Denmark
MEYER, Michael	European XFEL	Germany
Prof. MIKKELSEN, Anders	Lund University	Sweden
Dr. MILNE, Chris	Paul Scherrer Institute	Switzerland
Dr. MOBERG, Robert	Romo Scientific	Sweden
Prof. MÅRTENSSON, Nils	Department of Physics and Astronomy	Sweden
Dr. MÜLLER, Leonard	DESY	Germany
NEUTZE, Richard	University of Gothenburg	Sweden
Prof. NILSSON, Anders	Department of Physics, Stockholm University	Sweden
Prof. NILSSON, Carol	Lund University	Sweden
Prof. NORDGREN, Joseph	Department of Physics and Astronomy, Uppsala University	Sweden

NORDLUND, Dennis	SLAC National Accelerator Laboratory	United States
Prof. NORMAN, Patrick	Department of Physics, Chemistry and Biology	Sweden
ODELIUS, Michael	Stockholm	Sweden
Dr. OGASAWARA, Hirohito	SLAC National Accelerator Laboratory	United States
Mr. PARFENIUKAS, Karolis	KTH Royal Institute of Technology	Sweden
Dr. PATHAK, Harshad	Stockholms Universitet	Sweden
Dr. PATTHEY, Luc	Paul Scherrer Institut	Switzerland
Mr. PERAKIS, Fivos	SLAC national labs	United States
Dr. PERSHOGUBA, Sergey	NORDITA	Sweden
Dr. PERTSOVA, Anna	The Nordic Institute for theoretical physics	Sweden
Mr. PETTERSSON, Daniel	Fysikum, Chemical Physics	Sweden
Prof. PETTERSSON, Lars G.M.	Department of Physics, Stockholm University	Sweden
Prof. PUGLIA, Carla	Dept. of Physics and Astronomy, Uppsala University	Sweden
Mr. QUITMANN, Christoph	MAX IV Laboratory, Lund University	Sweden
RAHOMÄKI, Jussi	KTH Royal Institute of Technology	Sweden
Mr. REBROV, Oleksii	Stockholm University	Sweden
RENSMO, Håkan	Uppsala University	Sweden
Mr. REUTZEL, Marcel	Physics Departement, Philipps-University Marburg	Germany
RUBENSSON, Jan-Erik	Institutionen för fysik och Astronomi	Sweden
Mrs. SAAK, Clara	Uppsala University	Sweden
Dr. SALAZAR-ALVAREZ, G.	Stockholm University	Sweden
Dr. SALEN, Peter	Stockholm University	Sweden
Dr. SASSA, Yasmine	Uppsala University	Sweden
Dr. SCHERZ, Andreas	European XFEL	Germany
Prof. SCHNADT, Joachim	Division of Synchrotron Radiation Research, Lund University	Sweden
Dr. SCHOENLEIN, Robert	SLAC National Accelerator Lab	United States
Dr. SCHRECK, Simon	Stockholm University	Sweden
Prof. SELBERG, Jonas	KTH Royal Institute of Technology	Sweden
Prof. SKEPPSTEDT, Örjan	Fysikum	Sweden
Mr. SPÄH, Alexander	Stockholm University, Department of Physics	Sweden
Prof. STOHR, Joachim	SLAC/Stanford	United States
Prof. SUNDSTRÖM, Villy	Chemical Physics, Lund University	Sweden
Dr. THOMAS, Richard	Stockholm University	Sweden
THORIN, Sara	MAX-lab	Sweden
Dr. TIMNEANU, Nicusor	Uppsala University, Dept. of Physics and Astronomy	Sweden
Prof. TJERNBERG, Oscar	KTH	Sweden
Dr. UHLIG, Jens	Chemical Physics Lund University	Sweden
Dr. VAN DER MEULEN, Peter	Stockholm University	Sweden
Mr. VAZ DA CRUZ, Vinicius	KTH	Sweden
Prof. VOGT, Ulrich	KTH Stockholm	Sweden
Dr. WALSH, Noelle	MAX IV	Sweden
Dr. WASSDAHL, Nial	Uppsala University, Dep of Physics and Astronomy	Sweden
Dr. WEISSENRIEDER, Jonas	Material Physics, KTH	Sweden

Prof. WERIN, Sverker	Lund University/MAX IV	Sweden
Ms. WERNER, Josephina	Uppsala University	Sweden
Dr. WESTON, Matthew	Stockholm University	Sweden
Prof. WURTH, Wilfried	DESY/Universität Hamburg	Germany
Dr. YOUNG, Linda	Argonne National Laboratory	United States
Ms. ZHOU, Tunhe	KTH	Sweden
Prof. ÅGREN, Hans	Theoretical Chemistry and Biology, KTH	Sweden
Dr. ÖSTRÖM, Henrik	Stockholm University	Sweden

## B. Glossary

AMO	Atomic, Molecular and Optical science
APT	Attosecond Pulse Train
ASTRA	A Space charge TRacking Algorithm - particle tracking code
BOA	Born-Oppenheimer Approximation
CCD	Charged-Coupled Device
CHEM	Workshop break-up group devoted to chemistry
COND	Workshop break-up group devoted to condensed matter physics
CPP	Complex Polarization Propagator
D/A	Donar/Acceptor
DFT	Density Functional Theory
DICES	Doubly Intersecting Complex Energy Surfaces
EEHG	Echo-Enabled Harmonic Generation
Elegant	ELEctron Generation ANd Tracking – 6D accelerator program
FEL	Free Electron Laser
FemtoMAX	Femtosecond X-ray beamline at the SPF of MAX IV
FERMI	Free Electron laser Radiation for Multidisciplinary Investigations – FEL source at Trieste, Italy
FLASH	Free electron LASer in Hamburg
fs	femtosecond
Genesis	FEL simulation code
HDL	High Density Liquid
HGHG	High Gain Harmonic Generation
HHG	High-order Harmonic Generation
HOMO	Highest Occupied Molecular Orbitals
HIPPIE	MAX IV beamline focusing on Ambient pressure X-ray photoelectron spectroscopy
IR	Infra-Red
IT	Information Technology
KAW	Knut and Alice Wallenberg foundation
LCLS	Linac Coherent Light Source
LDL	Low Density Liquid
LIFE	Workshop break-up group devoted to life science
Linac	Linear accelerator
LLC	Lund Laser Centre
LLCP	Liquid-Liquid Critical Point
LLT	Liquid-Liquid Transition
LUMO	Lowest Unoccupied Molecular Orbitals
MLCT	Metal-to-Ligand Charge Transfer
MM	Molecular Mechanics
NanoMAX	MAX IV beamline for high spatial resolution experiments using hard X-rays
OPA	Optical Parametric Amplification
PALM	PhotoActivated Localization Microscopy
PES	PhotoEmission Spectroscopy
ps	picosecond
QM	Quantum Mechanics
RA	Resonant Auger

RIXS	Resonant Inelastic X-ray Scattering
SACLA	SPring-8 Angstrom Compact Free Electron Laser – X-ray FEL in Japan
SASE	Self-Amplified Spontaneous Emission
SAXS	Small-Angle X-ray Scattering
SEM	Scanning Electron Microscopy
SLAC	Stanford Linear Accelerator Center
SoftiMAX	MAX IV beamline for imaging using soft X-rays
SPF	Short Pulse Facility
SR	Synchrotron Radiation
SRIXS	Stimulated Resonant Inelastic X-ray Scattering
STM	Scanning Tunneling Microscopy
STXM	Scanning Transmission X-ray Microscopy
SwissFEL	Swiss X-ray FEL under construction at the Paul Scherrer Institute
SXL	Soft X-ray Laser
THz	Terahertz
Ti:Sa	Titanium:Sapphire
TOAS	Transient Optical Absorption Spectroscopy
UV	Ultra-Violet
VERITAS	MAX IV beamline for RIXS experiments
Vis	Visible
VUV	Vacuum Ultra-Violet
WAXS	Wide-Angle X-ray Scattering
XANES	X-ray Absorption Near-Edge Structure
XAS	X-ray Absorption Spectroscopy
XDS	X-ray Diffuse Scattering
XEOL	X-ray Excited Optical Luminescence
XES	X-ray Emission Spectroscopy
XFEL	X-ray Free Electron Laser
XMCD	X-ray Magnetic Circular Dichroism
XPS	X-ray Photoelectron Spectroscopy
XUV	Extreme Ultra-Violet
0D,1D,2D,3D	0,1,2,3-Dimensional, respectively